CZECH UNIVERSITY OF LIFE SCIENCES PRAGUE

FACULTY OF ENVIRONMENTAL SCIENCES

DEPARTMENT OF ENVIRONMENTAL GEOSCIENCES

ISOTOPIC FRACTIONATION OF CD AND ZN IN CONTAMINATED SOILS

DIPLOMA THESIS

THESIS SUPERVISOR: ING. ZUZANA VAŇKOVÁ, PH.D.

AUTHOR: BC. ŠÁRKA LEWANDOWSKÁ

2021

CZECH UNIVERSITY OF LIFE SCIENCES PRAGUE

Faculty of Environmental Sciences

DIPLOMA THESIS ASSIGNMENT

Bc. Šárka Lewandowská

Environmental Geosciences

Thesis title

Isotopic fractionation of Cd and Zn in contaminated soils

Objectives of thesis

The objective of literary research is to review the topic of isotopic fractionation, including analytical techniques used for its determination. The isotopic composition, and the mobility and availability of trace elements, especially Zn and Cd, will be summarized as well.

The first objective of the experimental part is to determine the concentrations of potentially available metals in the samples collected in the vicinity of Příbram smelting area. For this aim, diffuse gradients in thin film (DGT) and single extractions with 1 M KNO_3, 1 M CH_3COONa, and 0.005 M DTPA + 0.01 M $CaCl_2$ will be performed. The second objective is to assess the isotopic composition of Cd and Zn in the extracted solutions using the thermal ionization mass spectrometry (TIMS).

Methodology

1. Literary research is prepared using verified literary sources.

2. To obtain total concentrations of elements in samples, samples will be digested in aqua regia and hydrofluoric acid. To estimate the concentrations of potentially available metals in the study area, DGT and single extractions with three extracting agents (1 M KNO_3, 1 M CH_3COONa, and 0.005 M DTPA + 0.01 M $CaCl_2$) will be performed.

3. In order to determine the isotope variations of Cd and Zn between the mobile metal fractions and total content, measurements on thermal ionization mass spectrometer will be performed.

4. Results will be accompanied by appropriate discussion and the corresponding conclusions will be clearly assembled.

The proposed extent of the thesis

approximately 40-50 pages as needed

Keywords

soil contamination, isotopic fractionation, mass spectrometry, cadmium, zinc

Recommended information sources

EKMAN R., Silberring J., Westman-Brinkmalm A., Kraj A. [eds.], 2008: Mass Spectrometry: Instrumentation, Interpretation, and Applications. John Wiley & Sons, Inc., Hoboken.

KABATA-PENDIAS A. et Szteke B., 2015: Trace Elements in Abiotic and Biotic Environments. CRC Press, Boca Raton.

MEIER-AUGENSTEIN W., 2010: Stable Isotope Forensics: An Introduction to the Forensic Application of Stable Isotope Analysis. John Wiley & Sons, Inc., Hoboken.

NOVÁKOVÁ T., Kotková K., Elznicová J., Strnad L., Engel Z., Grygar T. M., 2015: Pollutant dispersal and stability in a severely polluted floodplain: A case study in the Litavka River, Czech Republic. Journal of Geochemical Exploration 156: 131-144.

POKROVSKY O. S., Viers J., Freydier R., 2005: Zinc stable isotope fractionation during its adsorption on oxides and hydroxides. Journal of Colloid and Interface Science 291: 192-200.

Expected date of thesis defence

2020/21 SS – FES

The Diploma Thesis Supervisor

Ing. Zuzana Vaňková, Ph.D.

Supervising department

Department of Environmental Geosciences

Electronic approval: 1. 3. 2021

prof. RNDr. Michael Komárek, Ph.D.

Head of department

Electronic approval: 2. 3. 2021

prof. RNDr. Vladimír Bejček, CSc.

Dean

Prague on 02. 03. 2021

Author's statement

I hereby declare that I have independently elaborated the diploma thesis with the topic of Isotopic fractionation of Cd and Zn in contaminated soils and that I have cited all the information sources that I used in the thesis and that are also listed at the end of the thesis in the list of used information sources.

I am aware that my diploma thesis is subject to Act No. 121/2000 Coll., on copyright, on rights related to copyright and on amendment of some acts, as amended by later regulations, particularly the provisions of Section 35(3) of the act on the use of the thesis.

I am aware that by submitting the diploma thesis I agree with its publication under Act No. 111/1998 Coll., on universities and on the change and amendments of some acts, as amended, regardless of the result of its defence.

With my own signature, I also declare that the electronic version is identical to the printed version and the data stated in the thesis has been processed in relation to the GDPR.

In Prague, 29 March 2021   …………………………………..

Acknowledgement

I would like to express my gratitude to the Department of Environmental Geosciences to let me participate in the research team and involve me in the project. Further, I would like to thank my supervisor Ing. Zuzana Vaňková, Ph.D., for the thoughtful comments and recommendations on this thesis. I am also thankful to everybody who has supported me throughout the editing of this work.

Abstrakt

Tato diplomová práce se zabývá mobilitou stopových prvků v kontaminované půdě a izotopickou frakcionací Cd a Zn, jež může poskytnout informace o biogeochemickém cyklu těchto kovů. V teoretické části jsou shrnuty poznatky z oblasti kontaminace půdy, izotopové a extrakční analýzy, a vybraných kovových kontaminantů – Cd a Zn (včetně jejich izotopické frakcionace).

V praktické části bylo zkoumáno 5 půdních vzorků odebraných z blízkého okolí Příbrami, která se v důsledku historické důlní a hutní činnosti potýká se zvýšeným znečištěním přilehlých půd a vodních toků. Pro každý ze vzorků byly určeny celkové koncentrace vybraných stopových prvků (As, Cd, Cu, Pb, Zn) a také jejich potenciální mobilita, která byla stanovena použitím různých extrakčních analýz – techniky DGT a jednoduchých extrakcí s následujícími činidly: 1 M KNO_3, 1 M CH_3COONa a 0.005 M DTPA s 0.01 M $CaCl_2$. Izotopové složení Zn a Cd v půdě a extraktech bylo zjištěno pomocí multikolektorového hmotnostního spektrometru s indukčně vázaným plazmatem (MC-ICP-MS) a hmotnostního spektrometru s termální ionizací (TIMS).

Výsledky ukázaly, že půdy byly obohaceny zejména Pb (až 16 907 ± 1 963 mg/kg). Další prvky se vyskytovaly dle sestupné celkové koncentrace v následujícím pořadí: Zn, As, Cu, Cd. Relativně nejmobilnějším prvkem bylo Cd, naopak nejméně mobilní byl As. Zatímco nejvyšší efektivitu k vyluhování prvků měla směs DTPA s $CaCl_2$, DGT technika byla schopna extrahovat pouze nejmobilnější frakci kovů. Izotopická data odhalila, že větší podíl těžších izotopů Cd se nacházel v extraktech ($\delta^{114/110}$Cd až 0.11 ± 0.06‰) v porovnání s půdou ($\delta^{114/110}$Cd od -0.24 ± 0.05‰ do -0.34 ± 0.03‰). Těžší izotopy Cd jsou patrně přednostně přerozděleny do půdního roztoku, kde jsou k dispozici pro rostliny. Obdobné výsledky byly získány u izotopů Zn, kromě lesních vzorků, u kterých byly lehčí izotopy Zn přednostně situovány v extraktu (např. $\delta^{66/64}$Zn půdy = -0.22 ± 0.03‰ vs $\delta^{66/64}$Zn DTPA-extraktu = -0.39 ± 0.00‰). Zajímavé je, že $\delta^{66/64}$Zn hodnoty získané po DGT extrakci (např. -0.29 ± 0.01‰) byly často ochuzeny o těžší izotopy ve srovnání jak s jednoduchými extrakcemi (např. $\delta^{66/64}$Zn = -0.06 ± 0.01‰ pro CH_3COONa-extrakt) tak s půdou (např. $\delta^{66/64}$Zn = -0.20 ± 0.01‰), což naznačuje, že lehčí izotopy Zn jsou pro rostliny dostupnější.

Klíčová slova:

kontaminace půdy, izotopická frakcionace, hmotnostní spektrometrie, kadmium, zinek

Abstract

This diploma thesis deals with the mobility and bioavailability of trace elements in contaminated soils and isotopic fractionation of Cd and Zn, which may provide insight into their biogeochemical cycling. The theoretical part summarizes information about soil contamination, isotopic and extraction analyses, and target metal contaminants, Cd and Zn, including their isotope fractionation.

The study investigated 5 soil samples collected in the vicinity of Czech town Příbram, known for its historical mining, processing, and smelting of polymetallic ores, resulting in pollution of surrounding soils and streams. The total metal(loid) concentrations and the potential mobility of selected elements (As, Cd, Cu, Pb, Zn) were determined using different extracting procedures (DGT technique, single extractions with 1 M KNO_3, 1 M CH_3COONa, and 0.005 M DTPA + 0.01 M $CaCl_2$). Moreover, the isotopic compositions of Zn and Cd in bulk soil and extracted solutions were investigated using multicollector-inductively coupled plasma mass spectrometry (MC-ICP-MS) and thermal ionisation mass spectrometry (TIMS), respectively.

Based on the total metal concentrations, the soils were particularly enriched with Pb (up to 16 907 ± 1 963 mg/kg), followed by (in order of decreasing concentration) the Zn, As, Cu, and Cd. Relatively the most mobile element was Cd, and the least mobile element was As. The highest extraction efficiency was obtained using a mixture of DTPA with $CaCl_2$. The DGT technique was able to extract just the most exchangeable metal pool. Isotopic data revealed that the Cd isotopes in the extracts were heavier ($\delta^{114/110}Cd$ of up to 0.11 ± 0.06‰) than those in the bulk soil ($\delta^{114/110}Cd$ of -0.24 ± 0.05‰ to -0.34 ± 0.03‰), suggesting that the heavier Cd isotopes are preferentially partitioned into the soil solution, thereby being available to plants. Similar results were obtained for Zn isotopes. However, forest samples showed the opposite results, with lighter Zn isotopes favourably distributed into the soil solution (e.g., soil $\delta^{66/64}Zn$ = -0.22 ± 0.03‰ vs DTPA-extract $\delta^{66/64}Zn$ = -0.39 ± 0.00‰). Interestingly, the $\delta^{66/64}Zn$ values obtained after DGT extraction (e.g., -0.29 ± 0.01‰) were mostly depleted in heavy isotopes in comparison to single extractions (e.g., $\delta^{66/64}Zn$ = -0.06 ± 0.01‰ for CH_3COONa extract) and bulk soil (e.g., $\delta^{66/64}Zn$ = -0.20 ± 0.01‰), suggesting that lighter Zn isotopes are more available to plants.

Keywords:

Table of Contents

1. INTRODUCTION

Environmental pollution is a serious ongoing problem. It can be defined as a release of energy and substances into the environment, which may have a detrimental effect on the lives and health of people and animals, the ecosystems, and material property (Farmer 1997). Soil acts as a major sink for contaminants, gathering significant amounts of environmental pollution that end up in the soil from diverse anthropogenic and natural sources, for instance, industrial activity, waste disposal, sewage discharge, or volcanic activity. Since soil formation is a very slow process compared to the length of human life, it should be perceived as a non-renewable limited natural resource on which humankind is existentially dependent and which performs not only productive but also ecological and social functions in the landscape ecosystem.

Soil may become contaminated with potentially toxic metals, which, unlike organic compounds, do not degrade over time. Metal contamination often results from mining, disposal of waste, pesticide application, or combustion of fossil fuels. Common metals occurring on contaminated sites are Cd and Zn, which are a part of the same group in the periodic table because they have very similar electrons' arrangements in the outermost shells. Hence their properties are very similar (O'Neill 1998). However, while Zn is an essential micronutrient important for plant growth, harmful in excess amounts, Cd has toxic effects on soil biomass.

Assessing the type and extent of soil contamination has key importance in the context of risk assessment, remediation measures, and management of contaminated land. Environmental forensics is a scientific tool that uses various analytical techniques to examine contaminants in the environment. One of the methods is called stable isotope fingerprinting. Stable isotopes are found in diverse ratios depending on the origin and source. Distinct isotopic signatures (fingerprints) can be generated by isotope fractionation, i.e., depletion or enrichment of one isotope relative to another. Isotope fractionation processes include equilibrium fractionation (e.g., complexation, dissolution, precipitation) and kinetic fractionation (e.g., diffusion, evaporation) (Zhang et al. 2018). Hence, isotope fractionation can be used to study the sources and the mechanisms of metal translocation in soils.

Another important knowledge in the ecotoxicological assessment of contaminated soils is the concentration of trace elements, their mobility and bioavailability, which can be attained by applying various extraction procedures, such as single or sequential extraction methods, or diffusive gradients in thin films technique.

2. OBJECTIVES OF THE THESIS

The objective of literary research is to review the topic of isotopic fractionation, including analytical techniques used for the determination of isotopic composition. Summarised will also be the mobility and availability of trace elements, especially Zn and Cd, as common soil contaminants.

The first objective of the experimental part is to determine the concentrations of potentially available metals in the samples collected in the vicinity of Příbram smelting area using DGT technique and single extractions with three different extracting reagents (1 M KNO_3, 1 M CH_3COONa, and 0.005 M DTPA + 0.01 M $CaCl_2$). The second objective is to determine the isotopic composition of Zn and Cd in bulk soil and extracted solutions using multicollector-inductively coupled plasma mass spectrometry (MC-ICP-MS) and thermal ionisation mass spectrometry (TIMS), respectively.

3. LITERARY RESEARCH

3.1 Contamination

3.1.1 Contamination of soil

Soil contamination represents a broad category of degradation defined by the presence of toxic or other hazardous substances exceeding naturally occurring levels with a possible risk to human health or natural environments (Martinovský 2016). It may have a natural or anthropic origin.

Contamination of natural origin is associated with geochemical abnormalities related to geological factors – for example, rocks and minerals enriched with metals (e.g., Ni, Cr, and Cu in serpentine); or mining area and ore deposits – for example, sulphides containing toxic metals (e.g., Pb or Hg). Mining such material creates mine dumps that can spread over large areas instead of one original spot. Anthropic contamination, as its name would suggest, is originated from human activities. The sources of contaminants include, for example, urban waste disposal (leaching of landfills), industrial or agricultural activities (metallurgy, petroleum, power plants, the use of pesticides and fertilisers, …), atmospheric deposition caused by motor vehicles, and also war activities (presence of depleted uranium) (Bini 2010).

Contaminants can be divided into two categories – organic (e.g., mineral oil, aromatic compounds, combustion products) and inorganic chemical substances such as metals, radionuclides, anions (e.g., nitrates, phosphates), or volatiles (Bini 2010).

3.1.2 Potentially toxic metals and metalloids in contaminated soils

Potentially toxic or ecotoxic metals and metalloids that have been related to contamination are frequently classified as heavy metals. This term is based on their relatively high density and the assumption that all elements in this category and their compounds have highly toxic properties. However, one more specific definition, including a list of such elements, has not been generally accepted to this day. Therefore, it is better to avoid this term (Pourret et Bollinger 2018).

Metals and metalloids are a part of inorganic chemical contaminants, and those most commonly found at contaminated sites are As, Cd, Cr, Cu, Pb, Hg, Ni, and Zn. Although some metals are essential for plants and animals' growth in low concentrations as micronutrients, at higher concentrations, they represent a toxic threat to the environment. Metal contamination might also pose a risk to human health and the ecosystem due to bioaccumulation. Biomagnification of metals through the

food chain, their accumulation in plant and animal tissues increases the risk of toxicity in carnivorous animals and humans (Johnson et Singhal 2010).

Soils are a significant sink for metals released into the environment through emissions from animal manures, atmospheric deposition, coal combustion residues, disposal of high metal wastes, land application of fertilisers, leaded gasoline and paints, mine tailings, pesticides, rapidly expanding industrial areas, sewage sludge, spillage of petrochemicals, and wastewater irrigation (Asrari 2014).

Unlike organic compounds, which may microbially or chemically degrade over time, metals remain unchanged – they can only transform in terms of mobility, chemical form (speciation), and toxicity. Therefore, their total concentration in soils persists for a long time after their introduction (Johnson et Singhal 2010).

3.1.3 Environmental forensics

Environmental forensics is a discipline aimed at identifying the age and the source of a contaminant release from an environmental sample. Environmental forensics investigation includes several analytical methods and techniques used for the detection and identification of natural and anthropogenic sources of contaminants (Morrison et Murphy 2006).

Examples include aerial photo interpretation and photogrammetry, statistical methods, microscopy, contaminant transport modelling, microbiological techniques, mass spectrometry, or chromatography. Some environmental forensic methods are based on the analysis of stable isotopes or radioisotopes (Murphy et Morrison 2007).

3.2 Isotopes

Isotopes are atoms with the same number of protons and electrons but a different number of neutrons (Fig. 1). Atoms can be denoted by mass number (the sum of protons and neutrons) written as a superscript on the left of the element symbol (e.g., ^{12}C), and by atomic number (the number of protons/electrons) written as a subscript on the left of the element symbol (e.g., $_6C$). The number of neutrons can be calculated by subtraction of an atomic number from mass number (e.g., $^{12}_{6}C$: $12 - 6 = 6$ neutrons). Isotopes are usually denoted just by mass number, which is approximately equal to the relative atomic mass, as it allows easy determination of neutrons and protons in the atomic nucleus from the element symbol (Michener et Lajtha 2008).
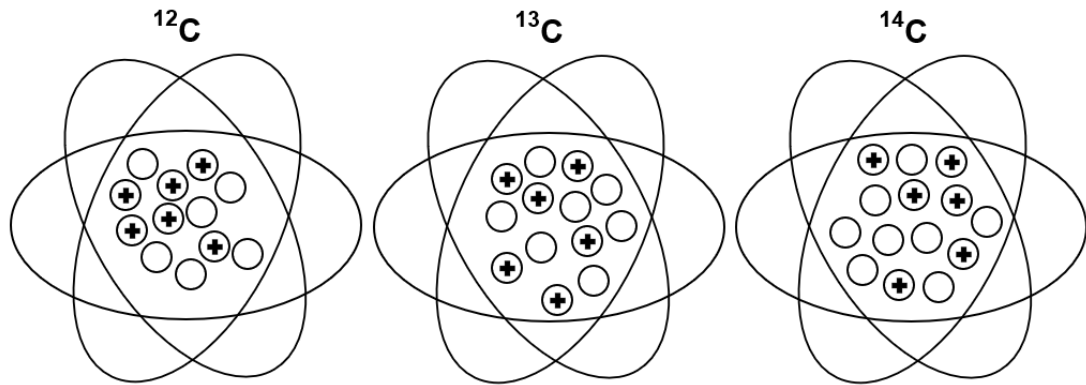
Fig. 1: Schematic diagram of three isotopes of carbon: ^{12}C and ^{13}C are both stable, ^{14}C is radioactive. Empty circles represent neutrons, circles with plus symbols represent positively charged protons, and ellipses represent the path taken by the six negatively charged electrons (not shown) as they orbit the atomic nucleus, balancing the charge of the protons (modified from Michener et Lajtha 2008).

There are two kinds of isotopes – radioactive and stable. Radioactive isotopes have an imbalance between the number of protons and neutrons. Therefore, they may undergo spontaneous radioactive decay – a process by which an unstable atomic nucleus loses energy due to the release of ionising radiation in the form of a particle (alpha and beta particles) or electromagnetic radiation (gamma, x-radiation) to reach a more stable state, transforming to a daughter isotope (possibly even different element). Some naturally occurring radioactive isotopes undergo fission after absorbing a neutron (e.g., ^{235}U) (Prasad 2012). Radioactive half-life is the time required for half of the radioisotopes in a substance to decay. For instance, if the half-life of million radioisotopes is one hour, most of the radioactivity will be gone in a few hours – after an hour, there will be half a million radioactive parent isotopes left and half a million new daughter isotopes generated. After another hour, there will be a quarter of a million parent isotopes and three-quarters of a million daughter isotopes and so on (Ellam 2016).

Conversely, stable isotopes appear to not decay over time. However, they may be produced as a result of the decay of radioactive isotopes. So far, approximately 3 500 isotopes have been discovered. Still, the majority have been found or made in laboratory experiments, and hence they do not naturally occur on Earth or only in trace amounts. The total number of stable isotopes is about 270, and the total number of radioisotopes may reach up to 6 000. All elements with atomic number greater than 83 are unstable and decay (Kirkland 2007, Konya et Nagy 2012).

3.2.1 Abundance, delta notation

In nature, elements usually occur as one predominantly abundant form of isotope (e.g., 98.93% of carbon in nature is present as ^{12}C and just 1.07% of carbon occurs

as ^{13}C). But the isotopic compositions in terrestrial environments slowly change through the processes of anthropogenic activities (e.g., testing of nuclear weapons, reactor accidents), cosmic ray interactions, radioactivity, and mass-dependent fractionations that accompany biological and inorganic reactions (Aelion et al. 2010).

Because the changes in isotopic composition at natural abundance levels are steadily minor, the isotopic composition of a sample is usually reported in delta notation (δ). That is expressed in units of permille (‰, one part per thousand) and calculated as a ratio of heavy to light isotope (e.g., $^{13}C/^{12}C$) in the sample and the designated isotopic standard, respectively (Fig. 2) (Hester et Harrison 2008).

$$\delta_S \ [‰] = \left(\frac{R_S}{R_{STD}} - 1\right) \times 1000 = \left(\frac{R_S - R_{STD}}{R_{STD}}\right) \times 1000$$

$$\text{e.g., } \delta^{13}C \ [‰] = \left(\frac{\left(\frac{^{13}C}{^{12}C}\right)_S}{\left(\frac{^{13}C}{^{12}C}\right)_{STD}} - 1\right) \times 1000 = \left(\frac{\left(\frac{^{13}C}{^{12}C}\right)_S - \left(\frac{^{13}C}{^{12}C}\right)_{STD}}{\left(\frac{^{13}C}{^{12}C}\right)_{STD}}\right) \times 1000$$

Fig. 2: Equation of delta notation (δ) calculation, where R_S is the measured isotope ratio in a sample and R_{STD} is the measured isotope ratio in the standard.

Delta values of natural samples typically range between -100‰ and +50‰. The negative delta value indicates a relatively less heavy isotope present in the sample than in the standard, and hence lower percentage of the heavy isotope is present in the sample. Conversely, if the delta value is positive, the sample is richer in the heavy isotope than the standard. The graph representing the relationship between abundance and delta value can be seen in Figure 3 (Fry 2007).
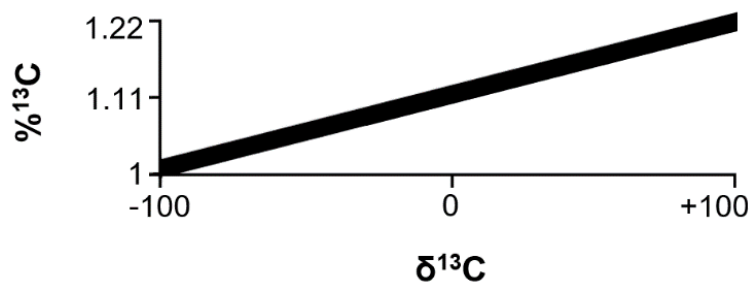
Fig. 3: Relationship of carbon isotope abundance to delta value; large natural delta variations from -100‰ to +100‰ correspond to slight variations in abundance of heavy isotope ^{13}C (%) (Fry 2007).

The difference in delta (δ) values, representing deviations from a standard, is described by the upper-case letter delta (Δ), called "big delta", which denotes the isotopic difference between a product and a reactant, two substances or two phases A and B: $\Delta_{A-B} = \delta_A - \delta_B$ (MacPherson et al. 2018).

The isotopic standard is an arbitrarily designated reference material used for reporting isotopic compositions. Each of the standards is, by definition, 0‰. Some of the original standards became exhausted and have been replaced by the new International Atomic Energy Agency (IAEA) standards with values similar to previous standards. Examples are shown in Table 1 (Meier-Augenstein 2010).

Tab. 1: Common delta reference materials (Meier-Augenstein 2010).

Element	Standard	Isotopic ratio	
Hydrogen	Vienna Standard Mean Ocean Water (V-SMOW)	$\frac{^2H}{^1H}$	0.0001558
Oxygen	Vienna Standard Mean Ocean Water (V-SMOW)	$\frac{^{18}O}{^{16}O}$	0.0020052
Carbon	Vienna Pee Dee Belemnite (V-PDB)	$\frac{^{13}C}{^{12}C}$	0.0112372
Nitrogen	Atmospheric air	$\frac{^{15}N}{^{14}N}$	0.0036765
Sulphur	Vienna Canyon Diablo Troilite (V-CDT)	$\frac{^{34}S}{^{32}S}$	0.0450045

3.2.2   Isotope effect

Isotopes have nearly identical chemical behaviour because the chemical reactions the atom undergoes are controlled by the number of electrons in an atom's outer shell. However, the physical properties may differ because the atomic mass determines the vibrational energy of the atomic nucleus. Therefore, the difference in atomic masses caused by a different number of neutrons affects reaction rate and bond strength. These differences of properties are called isotope effects, and they are especially noticeable among the lightest elements. For example, as shown in Table 2, water with ^2H has a slightly higher boiling point and density than water with ^1H (Michener et Lajtha 2008).

Tab. 2: Physicochemical properties of water of different isotopic composition; $^2H_2^{16}O$ is also known as heavy water (D_2O) (Hoefs 2015).

Property	$^1H_2^{16}O$	$^2H_2^{16}O$	$^1H_2^{18}O$
Density at 20 °C [g/cm^3]	0.9970	1.1051	1.1106
Temperature of greatest density [°C]	3.98	11.24	4.30
Melting point at 1 atm [°C]	0.00	3.81	0.28
Boiling point at 1 atm [°C]	100.00	101.42	100.14

The bonds formed by the heavy isotope are stronger than bonds involving the light isotope. Therefore, during a chemical reaction, molecules carrying the heavy isotope will generally react slightly less readily than those with the light isotope (Hoefs 2015).

3.2.3   Isotope fractionation

Isotope fractionation is the result of the dissimilar behaviour of isotopes. It refers to any situation which causes the different distribution of isotopes between two substances or two phases of the same substance with different isotope ratios. Thus, it changes the relative abundances of stable isotopes of an element. It can happen during biological, chemical, and physical processes. In general, the lighter elements (e.g., C, H, O, S) are more affected by isotopic fractionation than heavy elements. There are two main mechanisms causing fractionation: the kinetic isotope effect and the equilibrium (thermodynamic) isotope effect. Both of them are mass-dependent, which means that there is a measurable difference in the rates or level of the isotope fractionation, which is determined directly by the mass difference between the atoms or molecules involved (Gat 2010, Hoefs 2015).

3.2.4   Kinetic isotope effect

Kinetic isotope effect is the main phenomenon taking place in fast and irreversible (occurring in only one direction) reactions – such as diffusion and evaporation; or in any situation when equilibrium has not been completely reached. The main cause for this is the difference in reaction rates for the bond between two isotopes of the same element due to differences in bond strength, i.e., changes in bonding between the ground state and the transition state of reaction (activation energy) between two isotopes of different mass. The lighter compounds (containing isotopes with lower atomic mass) will form a weaker bond during kinetic fractionation and thus react faster than heavier compounds. As a result, the reaction products will always be depleted (reduced) in the heavy isotope relative to the reactants, which will be enriched with the heavier isotope. For instance, a $^{13}C^{16}O_2$ molecule with a mass of 45 g/mol will diffuse about 1.1% slower than the $^{12}C^{16}O_2$ molecule with a mass of 44 g/mol. Consequently, organic material originated by photosynthesis will be depleted in ^{13}C relative to air (Alexandre 2020, Lee 2012).

3.2.5   Equilibrium isotope effect

The equilibrium (thermodynamic) isotope effect is the second common isotope effect. It occurs in reversible reactions when two phases act with each other for a long period of time – when the equilibrium between phases (e.g., vapour vs liquid) or among chemical substances (reactant vs product) has been achieved in a reaction, the distribution of isotopes is different. It is related to the free energy change caused when one atom in a compound is replaced by its isotope. A compound with a heavier isotope in its composition has a smaller reserve of free energy compared to the same

compound containing the lighter isotope. As a result, in the analysed sample will occur differences in the physicochemical properties connected to vibration energy levels, for instance, boiling point, infrared absorption, melting point, molar volume and vapour pressure. For example, during the reaction between carbon dioxide and water in a closed container, the reactants and products remain in a short distance contact in a closed, well-mixed system so that back reactions are possible, and chemical equilibrium can be achieved: $C^{16}O_2 + H_2^{18}O \rightleftharpoons C^{18}O^{16}O + H_2^{16}O$. Here, the reactants and products are the same; however, the final masses are different from their initial masses because ^{18}O forms a stronger bond with carbon than ^{16}O does. Also, the physicochemical properties of $H_2^{18}O$ are different from $H_2^{16}O$ (as seen in Tab. 2). The greatest differences occur at low temperatures, which is currently used as a tool for studying past climate on Earth. In equilibrium fractionation, the heavier isotope tends to accumulate in the strongest bonds, for example, in the compound with larger molecular mass, in the denser phase, or in the phase with the highest oxidation state (Lee 2012, Michener et Lajtha 2008).

Isotopic fractionation (i.e., depletion/enrichment) can contribute to the determination of the source of material thanks to the formation of specific isotope ratio values that are characteristic of the origin, purity and manufacturing processes of the products and their components (Lee 2012).

3.2.6   Stable isotope fingerprinting

As already mentioned in Chapter 3.2.2 Isotope effect, two samples of the same chemical substance will, indeed, be chemically indistinguishable (same functional groups, chemical structure, constituent elements, etc.). However, the stable isotope analysis may lead to a distinction between these two samples if they do not share the same geographic origin or are derived from a different source and thus are isotopically distinguishable. For example, with the help of isotope profiling, it can be determined the source (the plant) and the origin (place in the world) of sugar samples (Tab. 3) (Meier-Augenstein 2010).

Tab. 3: Isotopic abundance of ^{13}C and ^2H in several sugar samples related to their source and geographic origin (Meier-Augenstein 2010).

| Source of sugar	Origin of sugar	$\delta^{13}C_{VPDB}$ [‰]	δ^2H_{V-SMOW} [‰]
Sugar beet	Poland	-25.42	-71.00
Sugar beet	Sweden	-26.84	-93.40
Sugar cane	Brazil	-11.76	-21.40
Sugar cane	South Africa	-11.10	-6.70

Another valuable use of isotope-ratio signature is to uncover evidence for criminal cases such as drug trafficking. Ehleringer et al. (2000) were able to determine cocaine

origin from different regions in South America by applying the stable isotope analysis combined with trace alkaloid data because cocaine carries a chemical fingerprint from the region where the coca plant was grown (Fig. 4).
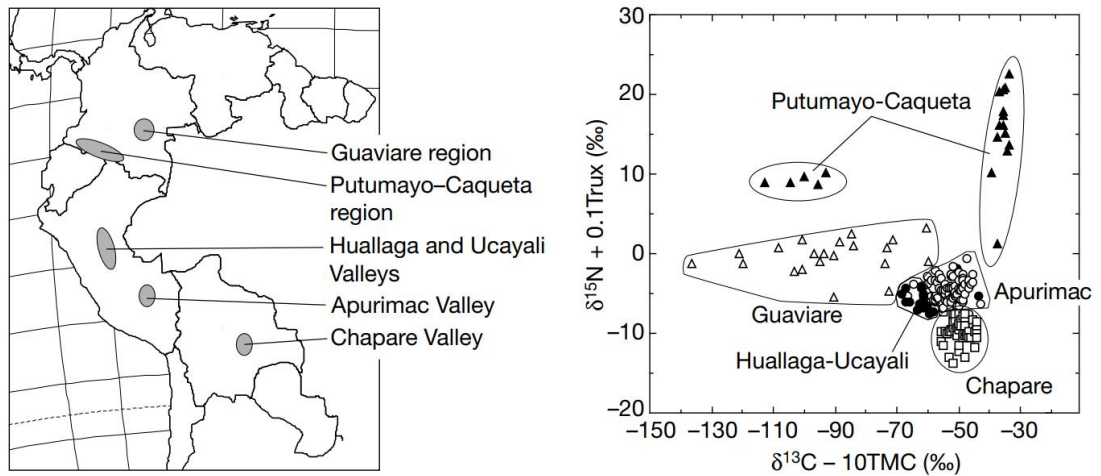
Fig. 4: Identification of cocaine-growing regions in South America (squares – Bolivia; triangles – Colombia; circles – Peru) based on trace alkaloid data (Trux – truxilline; TMC – trimethoxycocaine) in combination with C and N isotope ratios; standard for C is PDB and for N air (Ehleringer et al. 2000).

Stable isotope analyses can also be applied to trace the sources of pollution. In a study by Fang et al. (2018), authors were able to determine the predominant contribution of anthropogenic Pb inputs coming from unleaded vehicle exhaust particles, industrial activity (metallurgic dust), and fuel-burning (coal combustion), which were clearly distinct from leaded vehicle exhaust inputs (Fig. 5).
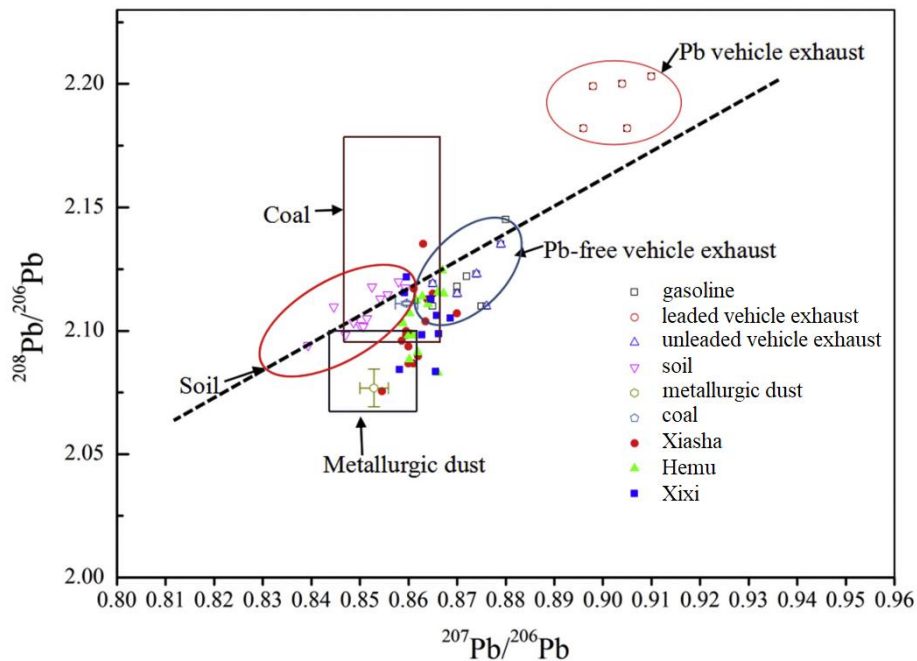
Fig. 5: Isotopic ratios of a Pb of the samples collected in Xiasha, Hemu and Xixi sampling sites and the isotope ratios ranges of different anthropogenic and natural sources in Hangzhou city, China; the dotted line represents Chinese ore lead line (Fang et al. 2018).

Therefore, stable isotope fingerprinting has a wide range of uses. It is useful when it is not possible to clearly determine the source of compounds based just on their presence. Stable isotopes can provide specificity in some cases. This technique depends on a difference in the relative proportion of light and heavy isotopes in compounds from different sources so that they may be distinguished from each other (Hester et Harrison 2008).

3.3   Mass spectrometry

Mass spectrometry (MS) is a highly sensitive analytical technique that measures mass-to-charge ratios (m/z) of ions formed from atoms or molecules in order to get information about elemental and molecular composition and also to quantify the abundance of individual chemical components. It can be used for the analysis of gaseous, liquid and solid samples (McCullagh et Oldham 2019).

The mass-to-charge ratio (m/z) is a dimensionless quantity. Although protons and electrons are electrically charged, their amount within an atom is equal; thus, their charges cancel out. An atom becomes charged when the number of protons is no longer equal to the number of electrons. For example, sodium atoms have 11 protons and 11 electrons, so the overall charge is 0. But sodium ions have 11 protons and 10 electrons, and thus the overall charge of the sodium ion is +1 (Holman et Stone 2001).

The relative atomic mass of an element can be found in the periodic table. It is the average weight of all its naturally occurring stable isotopes. For example, there are two stable isotopes of Cl – ^{35}Cl with the individual mass of 34.969 u (mass units) and the relative abundance of about 75.77%; and ^{37}Cl with the individual mass of 36.966 u and the relative abundance of around 24.23%. The average mass of Cl is calculated as 35.453 u based on individual masses and the natural occurrence of each isotope: [(75.77% x 34.969) + (24.23% x 36.966)] / 100% = 35.453 (Smith 2004).

A molecule of chlorine gas (Cl_2) can be formed either as $^{35}Cl_2$, $^{35}Cl^{37}Cl$ or $^{37}Cl_2$. Since the mass spectrometer responds to the masses of individual isotopes, no peak is observed at m/z 71 in the mass spectrum of the ionised forms of Cl_2. Instead, three determined ionic forms at m/z 70, 72 and 74 with the abundance of about 100, 64 and 10% respectively are reflected (Fig. 6) (Downard 2004).
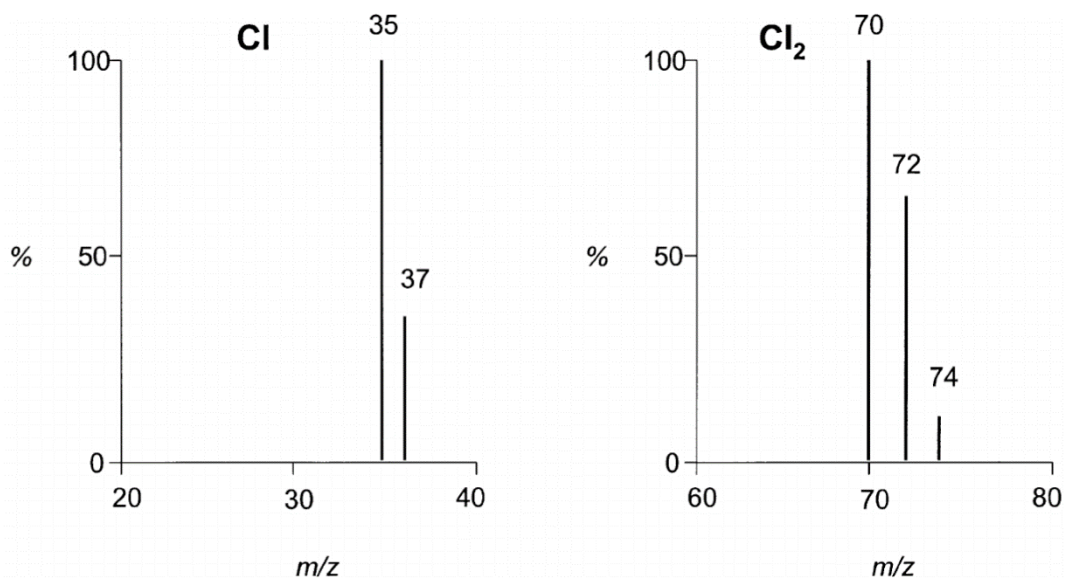
Fig. 6: Bar graph representation of mass spectra of atomic and molecular Cl. Note that the relative abundance (%) of the ^{37}Cl isotope is about one-third of ^{35}Cl, which corresponds to the relative abundances of these two isotopes (about 75% for ^{35}Cl and 25% for ^{37}Cl) (Downard 2004).

Every mass spectrometer consists of three main components: the ion source, the mass analyser, and the detector (Fig. 7). The mass analyser and the detector, as well as some types of ion sources, require vacuum for the operation to prevent collision with air molecules, so there is also a pumping system included (Misra 2019).
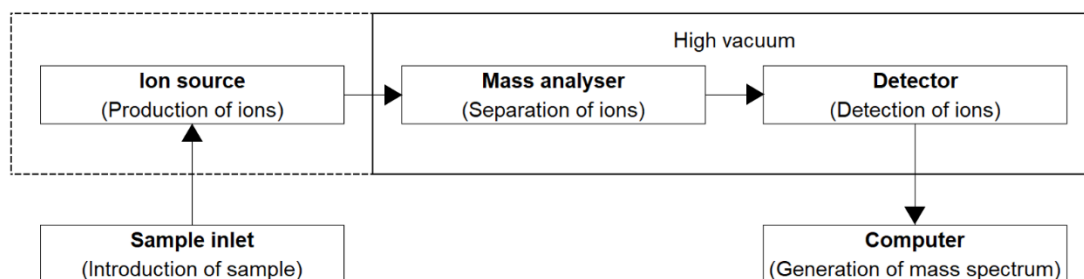
Fig. 7: Basic scheme of a mass spectrometer (modified from McCullagh et Oldham 2019).

Once the sample is introduced into the instrument via the inlet, it gets ionised in the ionisation chamber, extracted into the analyser, which determinates the ions based on their m/z. Lighter ions will be more deflected than heavy ones (Fig. 8). In the end, the ions are detected by detectors, and the mass spectra, including the relative abundance of each resolved ionic species, are documented. There is a large variety of different ionisation (e.g., electrospray, chemical ionisation, fast atom bombardment), separation (e.g., quadrupole, time of flight, ion trap) and detection (e.g., faraday cups, photomultipliers, microchannel plates) techniques (Misra 2019).
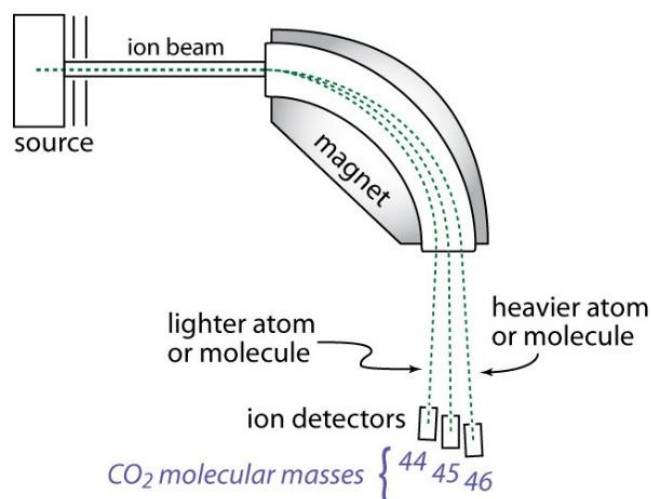
Fig. 8: Simple MS scheme depicting a triple-collector system arranged to analyse carbon dioxide, which is usually present in three different masses, depending on the isotopic composition: the most common variety is $^{12}C^{16}O_2$ with a molecular mass of 44 (SERC ©2007).

Different combinations of these techniques create different types of mass spectrometers. For example, mass spectrometers commonly used for the analysis of stable isotope composition of environmental samples are the Gas source isotope-ratio mass spectrometer (IRMS), Multicollector inductively coupled plasma mass spectrometer (MC-ICP-MS), and Thermal ionisation mass spectrometer (TIMS). All of these mass spectrometers have similar mass analysers made up of a magnetic sector (to produce mass spectrum) and multiple Faraday cups (to gather different mass ion beams at the same time), but they differ in sample introduction into the ion source and conversion of a sample into ions. Therefore, each of the instruments may be suitable for a different sample type (Aelion et al. 2010).

3.3.1   Isotope-ratio mass spectrometry (IRMS)

Isotope-ratio mass spectrometry (IRMS) is a general term for mass spectrometric methods which are used to measure the relative abundances of the different isotopes of an element in a sample. However, it is usually referred to as a gas source isotope ratio mass spectrometry. Gas source IRMS is traditionally used for the stable-isotope analysis of light elements (C, H, N, O, S), noble gases (He, Ne, Ar, Kr, Xe) and occasionally for Si and Cl. In this technique, the sample must be introduced in gaseous form. For example, in order to measure the isotopic composition of C in benzene, the compound has to be first transformed to the corresponding gas of measurement (e.g., CO_2). This sample gas is later compared to a reference gas calibrated using an international isotopic reference material with a well-defined isotopic composition (Prohaska et al. 2014).

13

The introduced gas molecules are ionised in electron ionisation (also known as electron impact) ion source. Ionisation is achieved by bombarding a beam of electrons (Fig. 9). A sample is introduced to the ionisation chamber through the sample inlet. The electron beam is formed by heating a Re or W filament with an electric current of 70 volts and after that collected in a trap electrode. Produced ions are electrically pushed out from the ion source to the analyser by the positive voltage on the repeller electrode (Ekman et al. 2008).
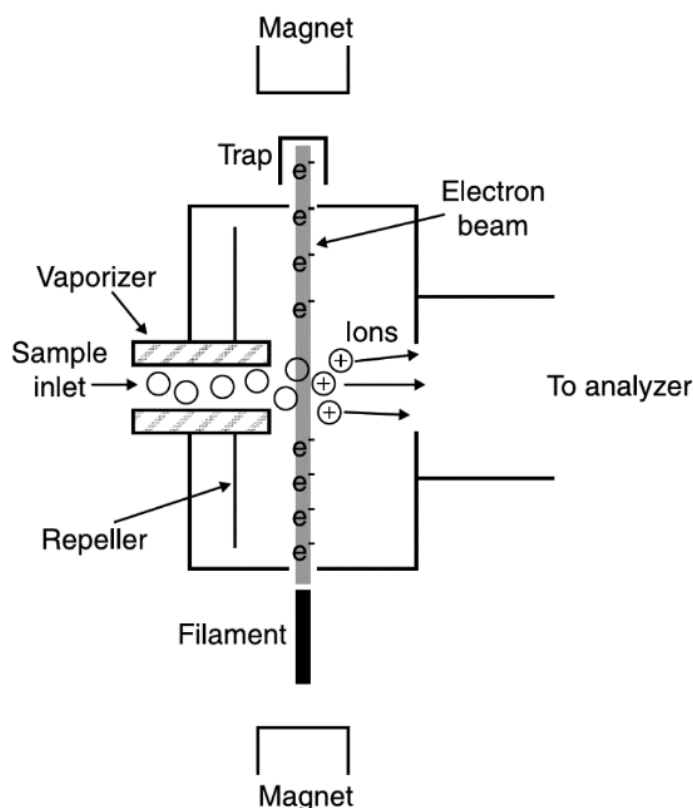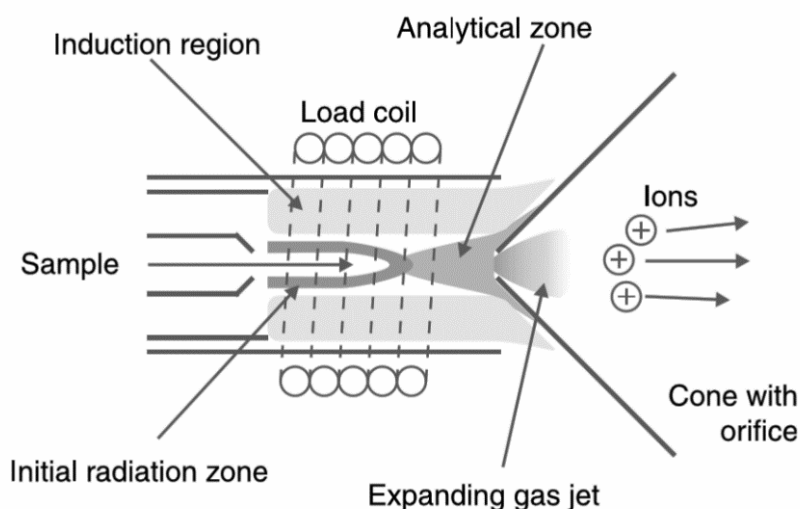

Fig. 9: Scheme of an electron ionisation ion source (Ekman et al. 2008).

3.3.2   Inductively coupled plasma mass spectrometry (ICP-MS)

In the inductively coupled plasma mass spectrometry (ICP-MS) the liquid samples are introduced through a nebuliser to create a fine aerosol that is afterwards moved to the high-temperature (up to about 7 700°C) Ar plasma. A plasma is an ionised gas containing positively charged ions and unbound electrons, allowing to atomise and ionise the sample. Generated ions are then extracted to a mass analyser (Wilschefski et Baxter 2019).

A typical ion source in ICP-MS (Fig. 10) consists of a quartz torch at the end of which the plasma is generated, and a load coil fed by radiofrequency energy to generate an oscillating magnetic field which accelerates and decelerates the ions and electrons of the plasma in order to heat the plasma inductively. There are several types of mass

spectrometers combined with an ICP source, for example, sector field mass spectrometers (ICP-SFMS) and multi-collector (MC-ICP-MS) instruments – these include multiple detectors (usually Faraday cups) for simultaneous detection of ions with different masses providing exceptional precision for isotope ratio measurements in the parts per million (ppm) range (White 2017).

*Fig. 10: Scheme of an inductively coupled plasma ion source (Ekman et al. 2008).*

Over 50 elements can be ionised with over 90% efficiency in ICP-MS with an Ar plasma. Only a few elements cannot be ionised because they have ionisation potential higher than Ar, for example, halogens (At, Br, Cl, F, I). In such cases, Ar may be replaced with He to provide better ionisation efficiency. This method is versatile and sensitive, often used for the analysis of inorganic compounds, including isotope ratio measurements and trace elements analysis (Ekman et al. 2008).

3.3.1 Thermal ionisation mass spectrometry (TIMS)

In thermal ionisation mass spectrometry (TIMS) are the ions produced thanks to electrical heating of one or more refractory metal filaments (such as Re, Ta, W) exposed to temperatures often exceeding 1 000 °C. Figure 11 illustrates the triple filament source. In such setup, the sample is manually loaded on one of the outer filaments, which is heated to evaporate the sample. Created neutral vapour is then directed towards a much hotter central filament, and the analyte is ionised and extracted to mass analyser and other parts of MS. The ionisation efficiency depends on the chemical and physical properties of the filament surface as well as the setup of filaments. The triple (or double) filament source may be a lot more effective compared to a single filament source because evaporation and ionisation are decoupled so that the ionisation filament can be subjected to higher temperatures. Therefore, even elements with high ionisation potential can be efficiently ionised. This

method represents a very precise, accurate and sensitive measurement of stable isotope ratios. Its main application is isotope analysis and geochronology (Ekman et al. 2008).
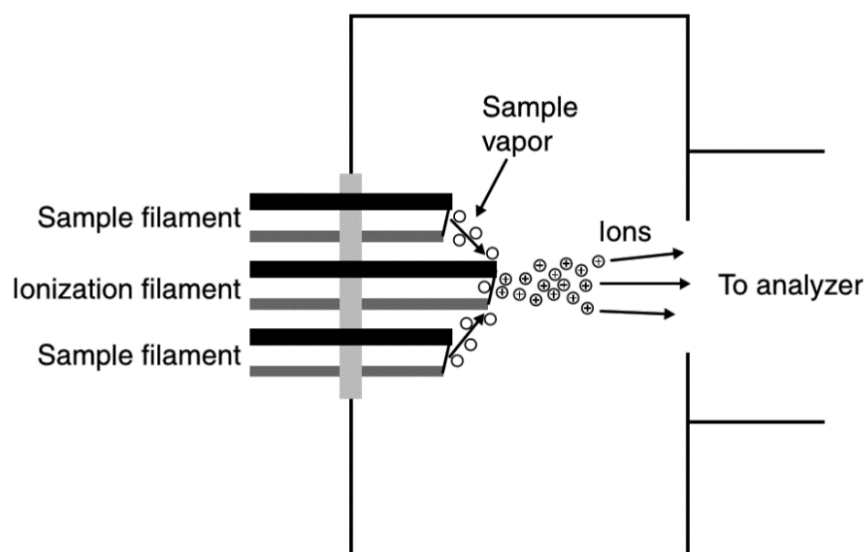

Fig. 11: Scheme of a thermal ionisation source with a triple filament setup; each filament consists of two pins connected by a wire (Ekman et al. 2008).

TIMS as well as MC-ICP-MS instruments allow isotope ratio measurements for numerous elements at precision below 50 ppm (parts per million). However, TIMS isotope analysis is more time-consuming because the sample must be manually loaded onto metal filament and carefully heated to gain a stable ion beam, while MC-ICP-MS has a simple automatic sample introduction. On the other hand, TIMS is less likely to be influenced by isotopic fractionation, which in MC-ICP-MS can be in the per cent range depending on instrument setting and time. Other differences between TIMS and MC-ICP-MS include running costs and element-specific advantages (Pico 2015).

3.4   Ion-exchange column chromatography

Chromatography is a general term for numerous techniques that allow the separation of different molecular species (analytes) from the rest of the components (matrix) in a sample. In general, the sample is introduced as a flowing mobile phase that moves through a stationary phase which retains passing species more or less according to the strength of their interaction with the stationary phase and releases them separately in time back into the mobile phase. Based on the used mobile phase, the following types of chromatography are recognised: liquid, gas, supercritical fluid, countercurrent and electrochromatography (Moldoveanu et David 2013).

Column chromatography is an adsorption method that is commonly used for the isolation and purification of individual components of interest present in the mixture. The mobile phase is liquid, and it acts as a solvent (introducing sample), developing agent (separating components) and eluting agent (removing separated components). In principle, the compound which needs to be separated is dissolved in the mobile phase and introduced from the top of the column. Components present in a mixture with a lower adsorption rate and lower affinity with the stationary phase compared to other components will move faster. Hence, they will be eluted out first, while the other components having a higher adsorption rate and more affinity with the stationary phase will be moving slowly and removed later. A schematic representation is shown in Fig. 12. There are several types of column chromatography based on the mechanism of separation: absorption chromatography, gel chromatography, ion-exchange chromatography, and partition chromatography (Akash et Rehman 2020).
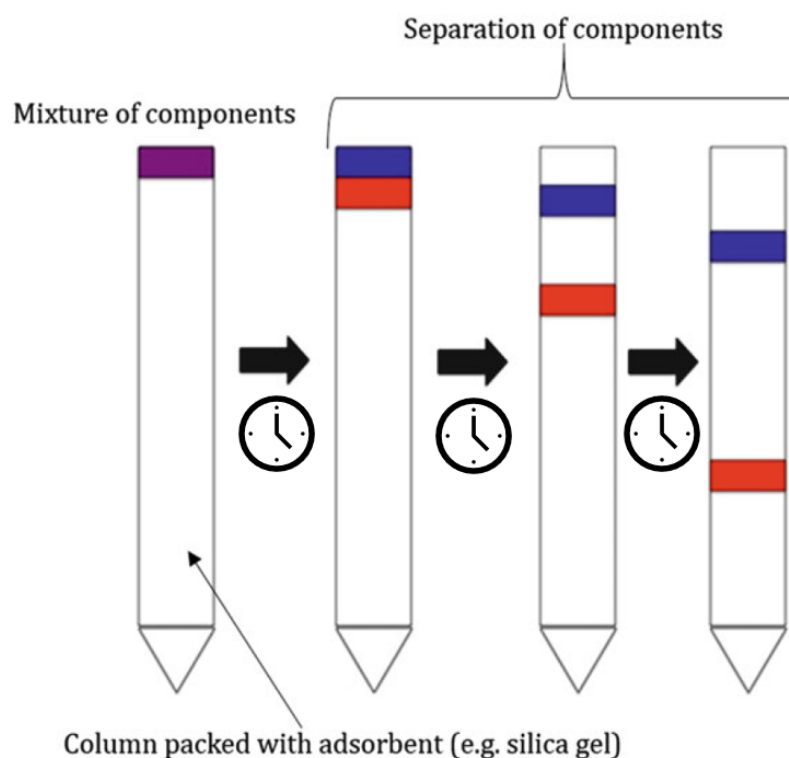

Fig. 12: Illustrative representation of column chromatography (modified from Akash et Rehman 2020).

Chemical separation of transition metals is frequently attained by ion-exchange column chromatography (Li et al. 2019). The separation in this technique is based on reversible electrostatic interaction between oppositely charged particles (ions), and it depends on the degree of attraction (affinity) of ions in the mobile electrolyte phase to the resin stationary phase. When the stationary phase (ion exchanger) carries a negative charge and attracts positively charged cations in the analyte, the process is referred to as cation-exchange chromatography. On the contrary, in anion-exchange

chromatography, the stationary phase bears a positive charge, and the exchangeable ions are negatively charged anions. Ion exchange material can be prepared either from naturally occurring biopolymers (e.g., cellulose) or from certain synthetic resins, which are insoluble porous organic molecules (Akash et Rehman 2020, Bisen et Sharma 2012).

Chemical separation and purification of Cd and Zn are commonly performed using anion-exchange column chromatography. Generally, the procedure begins with cleaning and conditioning of resin, onto which is later loaded the sample solution. After that, the elution (extraction of components adsorbed on resin) of the matrix elements (e.g., Ag, Al, Ca, Fe, In, and Pb) is carried out. Subsequently, the element of interest is eluted and collected, and the resin can be cleaned. The scheme of this procedure is depicted in Fig. 13. Each step of the process is performed using gravity flow of different eluents (carrier portion of the mobile phase, which moves the analytes with it) through resins contained in open columns. Acids of varying molar concentrations, such as hydrochloric acid (HCl), nitric acid (HNO$_3$) and hydrobromic acid (HBr) and their mixtures are usually used as eluents. As an anion exchange resin can be used for instance AG-MP-1 M, AG1-X8, or Eichrom TRU Spec (Li et al. 2019, Zhong et al. 2020).
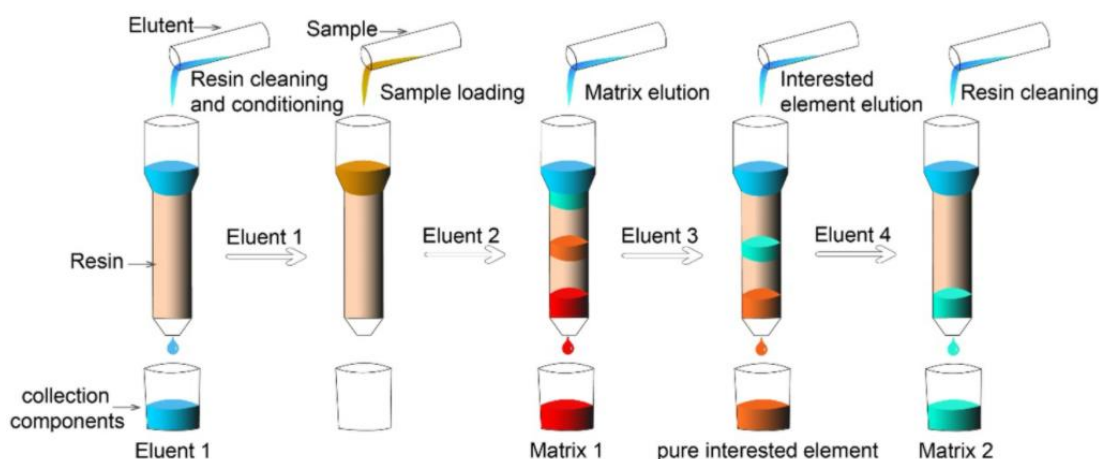
Fig. 13: Schematic representation of the chemical purification performed by ion-exchange chromatography; the eluents 1, 2, 3, and 4 may be the same (Li et al. 2019).

3.5 Extraction procedures for bioavailability assessment

Mobility of trace elements (e.g., Zn, V, Se, Ni, Mo, Pb, Cu, Co, Cr, Cd, B, and As) determines their environmental impact in contaminated soils. In unpolluted soils, trace elements are mostly present as comparatively immobile species in primary minerals (e.g., silicates, aluminates), which get gradually mobilised into forms available to plants due to the weathering. However, in polluted soils, trace elements often exist in

more labile forms (e.g., complexed, co-precipitated, sorbed), contributing to the pool of elements potentially available to plants and other living organisms. The determination of the different ways of trace elements binding in soils and sediments can provide valuable information on element mobility and availability, supplementing the total content data. There are many different analytical approaches, and some of them are based on leaching or extraction. Extraction tests are divided into single reagent (one extraction solution used for one soil sample) and sequential extraction procedures (several extraction solutions sequentially used for one sample) (Quevauviller 2002). Another approach is, for example, a relatively new technique called diffusive gradients in thin films (DGT).

3.5.1 Single extraction procedures

Single extraction procedures are widely recognised and frequently applied. It is a relatively simple and cost-effective technique providing reproducible results. Ideally, this method should be capable of mobilising and separating specific species (labile fraction) of trace elements representing their mobile (i.e., bioavailable, exchangeable) pool in soil. Generally, they can be categorised into the following groups (Hooda 2010):

- strong chelating solutions, e.g., diethylenetriamine pentaacetic acid (DTPA), ethylenediamine tetraacetic acid (EDTA)
- organic (weak) acids alone or combined acid-salt solutions, e.g., acetic acid (CH_3COOH), citric acid ($C_6H_8O_7$), oxalic acid ($H_2C_2O_4$), ammonium acetate (CH_3COONH_4), sodium acetate (CH_3COONa)
- diluted mineral acid solutions, e.g., hydrochloric acid (HCl), nitric acid (HNO_3), Mehlich-1 extracting solution (0.05 M HCl + 0.025 M H_2SO_4)
- unbuffered neutral salt solutions, e.g., ammonium nitrate (NH_4NO_3), calcium chloride ($CaCl_2$), magnesium chloride ($MgCl_2$), potassium nitrate (KNO_3), sodium nitrate ($NaNO_3$)

Diluted mineral acid extractants can extract nearly the whole amount of trace metals in soil depending on the strength and soil mineralogical composition. Chelating agents and diluted mineral acid solutions or combined acid-salt solutions are presumed to extract potentially mobile portions of trace metals. Methods using unbuffered neutral salt solutions were developed to simulate natural soil solutions; thus, they are useful for evaluation of ecological significance of trace elements (Kabata-Pendias 2010).

3.5.2 Sequential Extraction Procedures

As mentioned before, trace elements exist in different forms within soils – some may increase the risk of plant uptake (e.g., water-soluble), while other forms are relatively stable (e.g., bound to Fe and Mn oxides). The information on the movement and transformation of trace elements' forms have been considered potentially valuable for predicting their availability to plants. In the past, there have been proposed several sequential extraction procedures. In order to improve comparability between results, Standards, Measurements and Testing Programme of European Community (SM&T), formerly known as the Community Bureau of Reference (BCR), developed and defined sequential extraction procedure methodology. This BCR extraction is a three-step sequential extraction procedure that fractionates trace elements into three fractions: exchangeable (extraction step 1), reducible – bound to Fe and Mn oxides (step 2), oxidisable – bound to organic matter and sulphides (step 3) and the residual fraction, which can be determined directly or by the difference between the sum of the trace elements extracted in the three steps and their total amounts determined individually (Hooda 2010).

3.5.3 Diffusive gradients in thin films (DGT)

Traditional methods used for evaluation of metal bioavailability in soils – extractions with chemical reagents (e.g., DTPA, $CaCl_2$, NH_4NO_3) usually involve soil sampling, drying, grinding and treating with chemical solutions that can significantly modify the soil's conditions. Ideally, the test should minimally disrupt the equilibrium between solid and solution phases, which is sensitive to prevailing conditions (Naidu 2008). Diffusive gradients in thin films (DGT) is an exchange resin method, where the metal bioavailability is measured by being directly deployed on the surface of moist soil (CBCSS 2003).

The DGT device is a simple tight-fitting piston that consists of the binding resin layer, diffusive ion-permeable hydrogel and membrane filter (Fig. 14). In principle, metal ions diffuse through the membrane filter and upper permeable layer and are captured by the bottom binding layer that contains a resin embedded in a gel (typically acrylamide). Therefore, only labile metal species are trapped and gathered on the bottom resin layer (Karpas 2015). Metal distribution and flux for specific soils can be assessed by monitoring changes in solution concentration and the amount of metal adsorbed on the resin (CBCSS 2003).
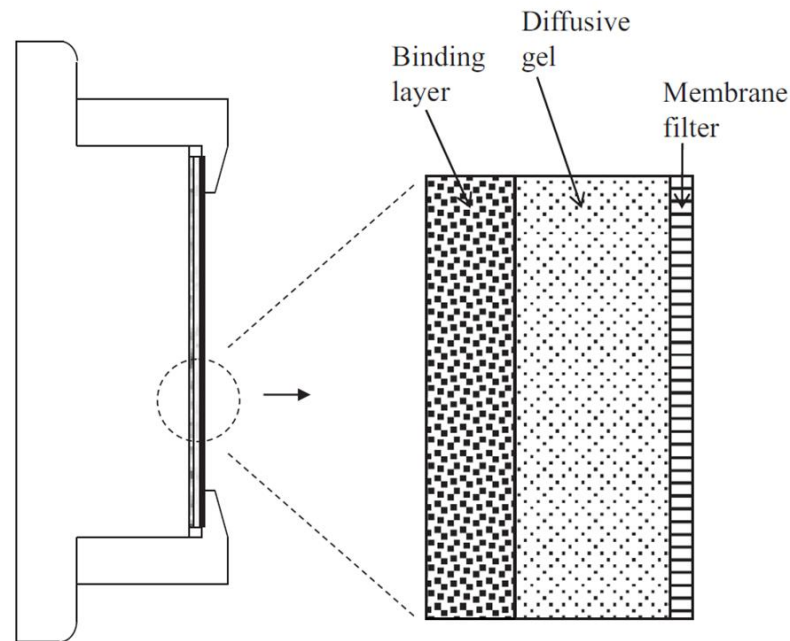
Fig. 14: Schematic representation of a DGT piston assembly, with an exploded view displaying binding layer, diffusive gel and membrane filter (modified from Davison 2016).

Newly established DGT method made of Zr oxide-based binding resin gel (ZrO-Chelex DGT) is capable of simultaneous measurement of cations [Cd(II), Co(II), Cu(II), Fe(II), Mn(II), Ni(II), Pb(II), Zn(II)] and oxyanions [As(III)/As(V), Cr(VI), Mo(VI), P(V), Sb(V), Se(VI), V(V), W(VI)] in various environmental matrices. This technique has a wide tolerance for ionic strength (2-3 mM to 750 mM) and pH (5-9) (Wang Y. et al. 2017).

Zhang et al. (2001) conducted a study in which they compared Cu uptake by pepperwort plants using DGT and other methods (e.g., conventional extraction with EDTA). Results demonstrated that DGT had the highest correlation coefficients with plant uptake concentrations compared to other traditional methods, implying that the DGT technique is more sensitive and robust in reflecting metal bioavailability in soils to plants.

3.6   Cadmium

3.6.1   Basic properties, soil content

Cadmium (Cd) is a white soft ductile flexible and malleable metal, part of group 12 in the periodic table of elements. Its atomic number is 48, and atomic weight is 112.41 g/mol. It naturally occurs in the earth's crust within a range of 0.1-0.5 mg/kg, and it is naturally present everywhere in the environment as a result of forest fires, volcanic eruptions, gradual process of abrasion and erosion of rocks and soil and other natural events. Common forms are inorganic salts, such as cadmium oxide

21

(CdO), cadmium chloride ($CdCl_2$), or cadmium sulphate ($CdSO_4$). However, the levels of Cd in the environment are changing due to contamination – estimated 25 000 to 30 000 tons of Cd are released each year, with major contributions coming from anthropogenic activities (e.g., application of fertilisers, burning of fossil fuels, mining, waste incineration, …) (Pappas et al. 2010).

In soils, Cd occurs at concentrations ranging from 0.06 to 1.1 mg/kg, with a worldwide average estimated at 0.41 mg/kg. The content of Cd in soils is primarily determined by parent materials. The highest concentrations are in calcareous (0.4-0.8 mg/kg) and organic soils (0.2-2.5 mg/kg). However, in soils derived from Cd enriched bedrocks, the concentration might reach up to about 8 mg/kg, even more in extreme cases. For instance, soils derived from altered pyritised andesine in Slovakia hold up to 222 mg/kg of Cd. Cd mobility is strongly affected by pH in all types of soils. Cd speciation in soil solutions varies depending on soil type. For example, in alkaline soils, Cd often occurs as hydrogen carbonate ($Cd(HCO_3)_2$). In oxic and acid soils, it can be present as $CdSO_4$, $CdCl_2$ or free Cd cation (Cd^{2+}), which is the most common form in soil solution, readily available to plants, occurring within a range of 55-90%. Soil microorganisms play an important role in Cd behaviour in soils because they have great capability to accumulate Cd (up to 1 120 mg/kg), and they can bond with Cd and later release it into the soil solution (Kabata-Pendias et Szteke 2015).

3.6.2 Discovery and production

Cd was discovered in 1817 by Friedrich Stromeyer when he heated a sample of calamine (zinc carbonate, $ZnCO_3$), commonly used as medicine in the 19th century, and expected colourless reaction. But an unknown metallic impurity would change colour. Subsequently, he extracted new metal similar to Zn and named it "cadmium" after "cadmia" which is a Latin word for calamine (Cobb 2008).

Although Cd is estimated as the 65th most abundant element, which is more than Ag or Au, it is not present as a free metal in nature. It can be found in a mineral called greenockite (cadmium sulphite, CdS). This ore, as well as other Cd minerals, is rare, and the concentrations of Cd are not high enough to be mined profitably. However, Cd is also associated with other metallic (Zn, Pb or Cu) ores (Krebs 2006).

Today is most Cd metal obtained as a by-product from the processing and refining of Zn ores and concentrates. For example, economically the most important Zn ore mineral (sphalerite) contains minor amounts of Cd. The main production of primary Cd metal takes place in Asia – leading producers in 2019 were China (8 200 t), the Republic of Korea (5 000 t) and Japan (1 900 t). Other countries which produce Cd

include Canada, Mexico, Kazakhstan, Netherlands, Russia and Peru. A smaller amount of secondary Cd metal is recovered from recycled consumer and industrial nickel-cadmium batteries, which presumably account for most of today's global Cd consumption. Other uses for Cd and its compounds comprise semiconductors for solar cells, plastic stabilisers, paint pigments, anticorrosive coatings, and alloys (USGS 2020).

3.6.3 Toxicity

Unlike Zn, Cd is not an essential element for life. In fact, it is considered as one of the most ecotoxic metals that exhibit very harmful effects on all biological processes. The toxicity is caused by metal replacement – Cd replaces Zn in important enzyme molecules making them inactive. The amount of Cd in an organism increases with age – at the age of 50, it is around 20 mg for the average human body (70 kg). About half of this amount is accumulated in kidneys, about 15% in the livers and around 20% in muscles. For adults, the account for Cd absorption from the diet is about 1-10%. The highest quantity of Cd in dietary is given by potatoes and cereals (mean 0.021 mg/kg). However, smoking 20 cigarettes a day leads to a greater Cd uptake in the body than the daily absorption from food. Estimated biological half-live is ranging from 10 to 33 years. Cd is absorbed in the lungs and guts, and the blood transports it to the liver and kidneys, where it is bound and retained to special enzyme metallothionein. Thanks to this enzyme, the body can endure Cd to a certain extent. Nevertheless, after high intakes, Cd can destroy the kidneys and lungs' functions and soften the bones, leading to severe pain (Enghag 2004, Kabata-Pendias et Szteke 2015).

The International Agency for Research on Cancer (IARC) classified Cd and its compounds as carcinogenic to humans with sufficient evidence for lung cancer. Because some less toxic alternatives can substitute Cd in some applications, the use of Cd has been restricted by law in several countries. For instance, nickel-cadmium batteries can be replaced by lithium-ion and nickel-metal hydride batteries, calcium-zinc or barium-zinc plastic stabilisers can replace barium-cadmium stabilisers in flexible polyvinyl chloride (PVC) applications, and cerium sulphide offers a non-toxic alternative to Cd pigments (USGS 2020).

3.6.4 Isotopes

Cd has 41 known isotopes, ranging from ^{94}Cd to ^{134}Cd. Most of them are artificially produced and radioactive with a half-life of less than 1 hour. In nature, Cd occurs as eight isotopes shown in Table 4. Two of them are radioactive with extremely long

half-lives, 8.04×10^{15} years for ^{113}Cd and 3×10^{19} years for ^{116}Cd. ^{114}Cd is the most abundant isotope and accounts for almost 29% of Cd atoms (Holden et al. 2018).

Tab. 4: Isotopes of Cd, their relative atomic mass and abundance. Isotopes denoted with a radioactive sign (☢) are radioactive, the half-lives of ^{113}Cd and ^{116}Cd are 8.04×10^{15} years and 3×10^{19} years, respectively (Holden et al. 2018).

Isotope	Relative atomic mass	Abundance [%]
^{106}Cd	105.906	1.245
^{108}Cd	107.904	0.888
^{110}Cd	109.903	12.470
^{111}Cd	110.904	12.795
^{112}Cd	111.903	24.109
^{113}Cd ☢	112.904	12.227
^{114}Cd	113.903	28.754
^{116}Cd ☢	115.905	7.512

The most frequently measured isotope ratio is ^{114}Cd/^{110}Cd because there is a considerable difference in atomic masses, and both isotopes have abundances over 10%. Delta values for ^{114}Cd/^{110}Cd in terrestrial materials range from -3.6‰ to +3.4‰. The primary isotopic reference material is BAM-I012. Unfortunately, this standard is isotopically fractionated relative to the mean Earth's crust by -1.3‰. Therefore, the scientists are searching for new zero-delta material, suggested is Cd-2211 which is not commercially available yet. Meanwhile, it can be replaced with NIST SRM 3108, which meets the criteria. There are also several secondary standard alternatives from local laboratories, such as Alfa Cd Zürich, JMC Cd Mainz, JMC Cd Münster, and Münster Cd. But most of these are not available as a general worldwide resource (Brand et al. 2014).

3.6.5 Isotope fractionation

Isotope variation of Cd is mainly caused by two fractionation processes. The first is biological uptake and utilisation of Cd in the seawater column, which can be used to study marine biological activity changes in the past. Large Cd isotopic variations also result from incomplete evaporation or condensation processes in extra-terrestrial materials and refining ore minerals. Soil sampled close to ore refineries might be enriched in Cd concentration displaying characteristic delta values. Measurable isotope fractionations of Cd usually occur during coal burning, smelting of Zn and Pb ores, and sulphide smelting and refining. Therefore, Cd isotopes can act as valuable tracers for anthropogenic sources of Cd into soils. The range of reported delta values of $^{114/110}$Cd given relative to SRM 3108 are presented in Figure 15 (Hoefs 2018, Teng et al. 2017).
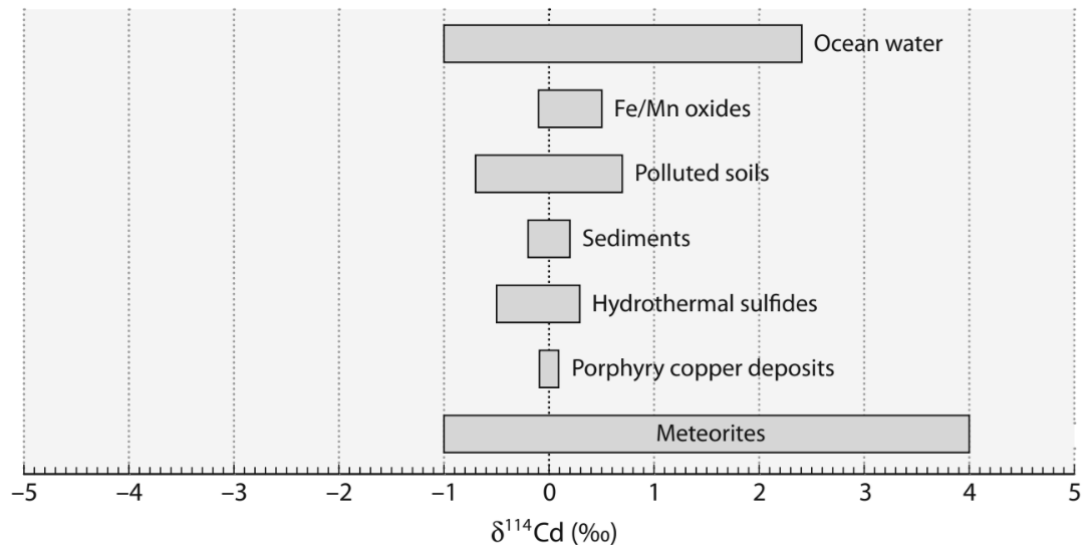
Fig. 15: Delta values for $^{114/110}Cd$ of important geological reservoirs (Hoefs 2018).

In the soil-plant system, the movement of Cd mainly comprises transport within plants, transport in the rhizosphere, and root uptake, which has crucial importance for the determination of the isotopic composition of the whole plant. Generally, shoots are likely to be enriched in the heavier Cd isotopes compared to roots. The sorption of Cd by soil minerals can have an effect on metal mobility and the isotope fractionation between soil solution and soil solid phases. Soil minerals tend to adsorb light Cd isotopes and by that causing an enrichment with heavy isotopes in the soil solution (Zhang et al. 2018).

Zhu et al. (2018) investigated Cd isotope compositions in different secondary minerals. Results suggest that light Cd isotopes are preferentially enriched during weathering in samples with small particle sizes, which indicate that particle size may significantly influence Cd isotope fractionation. The following trend in light Cd isotope enrichment was found: anglesite ($\delta^{114/110}Cd \approx$ -0.57 ± 0.03‰) > small particle granular smithsonite ($\delta^{114/110}Cd \approx$ 0.04 ± 0.14‰) > large particle granular smithsonite ($\delta^{114/110}Cd \approx$ 0.15 ± 0.40‰) > hydrozincite ($\delta^{114/110}Cd \approx$ 0.26 ± 0.01‰).

Wasylenki et al. (2014) studied Cd isotope fractionation during adsorption to Mn oxyhydroxide (synthetic birnessite) at low and high ionic strength. Authors reported that at low ionic strength, a small fractionation effect occurred ($\Delta^{114/112}Cd_{fluid-solid}$ = +0.12 ± 0.06‰), which was constant as a function of the fraction of total Cd sorbed, demonstrating a reversible equilibrium isotope effect. Average fractionation $\Delta^{114/112}Cd_{fluid-solid}$ = +0.27 ± 0.07‰ was observed at high ionic strength. A time-series carried out at high ionic strength disclosed that the extent of isotopic fractionation decreases gradually over time, from $\Delta^{114/112}Cd_{fluid-solid}$ of almost +0.4‰ after 1 h to +0.2‰ after 24 h and +0.1‰ after 912 h while the percentage of Cd sorbed to

birnessite increased from 27% to 58%. That might be explained by changes in the structure and crystallinity of birnessite over time and/or the change in the molecular mechanism of Cd sorption on birnessite.

3.7   Zinc

3.7.1   Basic properties, soil content

Zinc (Zn) is, just like Cd, also a transition metal, part of group 12 in the periodic table of elements. Because of their similar electron configuration and ionisation potential, they have similar geochemical behaviour. The atomic number of Zn is 30, and the atomic weight is 65.41 g/mol. Zn is lustrous bluish-white malleable and ductile metal, i.e., it can be hammered into different shapes without breaking and stretched into wires (Tobler 2019).

In the earth's crust, Zn occurs within a range of 50-80 mg/kg; on average, it is about 75 mg/kg. The mean content of Zn in soils worldwide ranges from around 30 to 100 mg/kg – the amount is closely related to soil texture, and usually, the lowest amount is in light sandy soils (30-50 mg/kg). Conversely, Zn concentration might be elevated in calcareous and organic soils, ranging between 50-100 mg/kg for both soil types. The mobility of Zn in most soils is controlled by clay minerals, hydrous oxides, soluble organic matter content and pH. Both clay fraction and organic matter have a great sorption capacity for Zn. Therefore, they influence the accumulation of Zn in surface soil horizons. Zn is very mobile in acidic sandy soils and easily leaches down the soil profiles. The most common and mobile Zn species, present mainly in soil solutions, are zinc hydrogen carbonate ($Zn(HCO_3)_2$) and zinc hydroxide (ZnO_2). Other compounds include zinc ferrite ($ZnFe_2O_4$), zinc phosphate ($Zn_3(PO_4)_2$), and zinc carbonate ($ZnCO_3$). Anthropogenic sources of Zn include industrial activities (e.g., smelting), traffic, and agricultural practise (e.g., fertilisers, pesticides) (Kabata-Pendias et Szteke 2015).

3.7.2   Discovery and production

Zn was discovered as an element in 1746 by Andreas Marggraf. However, people were using Zn ores long before to make brass (an alloy of Cu and Zn). The earliest brass items date back to ancient Greece and Rome era over 2 000 years ago (Gray 2006).

Zn is the 24th most abundant element on Earth. Naturally, it is not present in pure metallic form but associated with other elements in several minerals, such as franklinite ($ZnFe_2O_4$), hydrozincite ($Zn_5(CO_3)_2(OH)_6$), smithsonite ($ZnCO_3$), willemite

(Zn_2SiO_4), wurtzite ($(Zn, Fe)S$), and zincite ($(Zn, Mn)O$). But the most important Zn ore is mineral sphalerite, also known as zincblende (zinc sulphide, ZnS) (Krebs 2006).

Total global resources of Zn are estimated to be around 1.9 billion tons. In 2019 the worldwide mine production (roughly 13 million tons) increased by an estimated 4% compared to 2018. Significant Zn producers in 2019 were China (4.3 million t), Peru (1.4 million t) and Australia (1.3 million t). Other countries which produce Zn include India, USA, Mexico, Bolivia, Russia, Canada, Kazakhstan, and Sweden. Most of the consumed Zn was used to galvanise other metals (e.g., iron to prevent rusting), followed by zinc-based diecasting alloys and brass, and other chemical, electronic, and pigment use (USGS 2020).

3.7.3 Importance of Zn

Zn is an essential trace element for organisms to function correctly. It is a part of many metabolic enzymes, contributes to the production of insulin in the pancreas, and is significant for DNA and RNA replication. A small quantity of Zn is contained in each cell of the body, but over 90% of the Zn is present in bones and muscles. Zn keeps the immune system strong, protects from diseases and infections, and also promotes skin cell renewal. Deficiency of Zn leads to hair loss, skin problems (e.g., acne), white spots on nails, loss of sense of smell or appetite, and impaired wound healing. Furthermore, a Zn deficiency may cause delayed mental development, retarded growth and postponed puberty for children. Recommended daily intake of Zn is 8 to 11 mg depending on age and gender, which corresponds approximately to 0.15 mg per kilogram of body weight. The best source with high Zn content in the diet is red meat – beef contains about 4 mg per 100 g. Other dietary sources containing high amounts of Zn are fish, poultry, seafood, offal, whole-wheat bread, sunflower and pumpkin seeds, bran, maple syrup and brewer's yeast. On the contrary, fruits generally have low Zn contents (0.15 mg per 100 g). Although Zn is essential for life, excess Zn can be harmful and lead to stomach cramps, vomiting, diarrhoea, or fever (Enghag 2004, Tobler 2019).

3.7.4 Isotopes

Zn has 32 known isotopes, ranging from ^{54}Zn to ^{85}Zn. Most of them are artificially produced and radioactive, with a half-life of less than 1 hour. In nature, Zn occurs as five isotopes shown in Table 5. ^{64}Zn is the most abundant isotope and accounts for almost half of the Zn atoms. Since the stable isotopes have slightly different properties, they can be fractionated during biological, chemical, or physical processes leading to variations in isotopic abundances. Stable isotopes of Zn have been used

as environmental tracers to investigate chemical and biogeochemical processes in contaminated sites in the environment. For example, the isotope ratio $^{66}Zn/^{64}Zn$ can be used as a tracer for detecting anthropogenic Zn pathways (Holden et al. 2018).

*Tab. 5: Isotopes of Zn, their relative atomic mass and abundance (Holden et al. 2018).*

Isotope	Relative atomic mass	Abundance [%]
^{64}Zn	63.929	49.17
^{66}Zn	65.926	27.73
^{67}Zn	66.927	4.04
^{68}Zn	67.925	18.45
^{70}Zn	69.925	0.61

The most commonly measured isotope ratios in stable isotope studies are $^{68}Zn/^{64}Zn$ and $^{66}Zn/^{64}Zn$. Naturally, the isotopic variations are relatively small, exhibiting a range of only ~1‰ for $\delta^{66/64}Zn_{IRMM-3702}$ measurements. Therefore, the precision of measurement must be very high. The first reference material was JMC Lyon, and it is now exhausted. Since 2006 there has been available new standard IRMM-3702 which should be used as the zero-delta for both aforementioned isotope ratios. Other reference materials are, for example, IRMM-651 and IM-1009 (Brand et al. 2014).

3.7.5   Isotope fractionation

Isotope variation of Zn is mainly caused by two fractionation processes: sorption processes; and evaporation-condensation processes, where the solid phase is enriched in the heavier isotopes compared to the vapour phase, which is depleted in the heavier isotopes. Rather than being found as a free metal ion, almost all of the Zn in the soils, rivers, and oceans is sorbed onto surfaces of clays and oxyhydroxides or organically complexed. The extent of isotope fractionation generally depends on the structure of Zn complexes on the solid's surface. Isotope fractionation of Zn during sorption on the organic matter depends on pH and the type of organic matter. Natural isotopic variations of Zn, given as $^{66/64}Zn$ ratios, are presented in Figure 16 (Hoefs 2018, Teng et al. 2017).
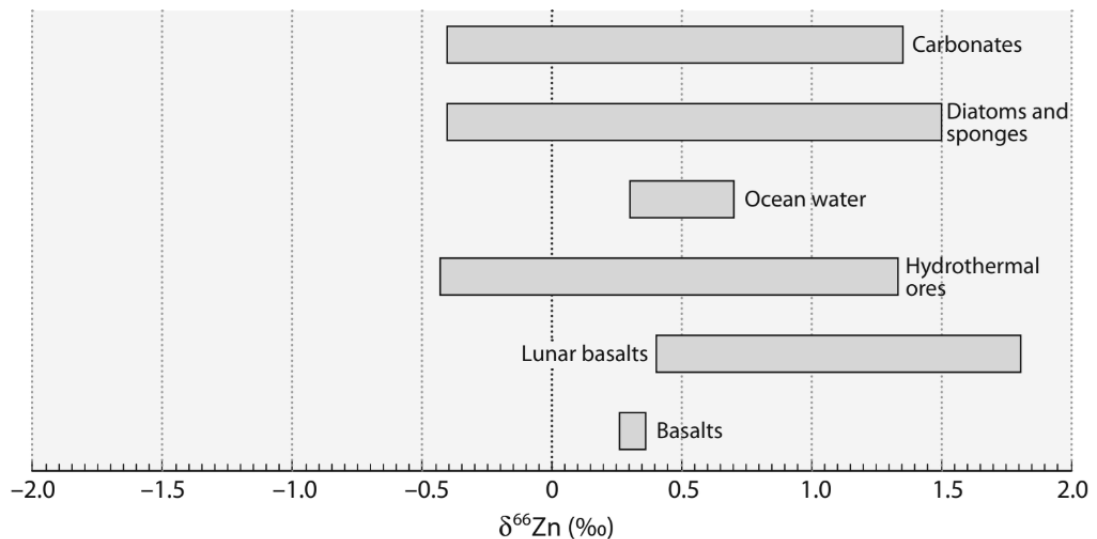
Fig. 16: Delta values for $^{66/64}$Zn of important geological reservoirs (Hoefs 2018).

In the soil-plant system, the movement of Zn involves mostly the same transport processes as Cd (transport within plants, transport in the rhizosphere, and root uptake). The plants are typically enriched with heavy Zn isotopes relative to soils. Moreover, roots are usually isotopically heavier than shoots. Additionally, the leaves get gradually depleted of the heavier isotopes with increasing height. The main sources of Zn fractionation are sorption (adsorption and desorption), diffusion, low- and high-affinity transport phenomena, and speciation. The sorption of Zn by soil minerals can influence the metal mobility and the isotope fractionation between soil solution and soil solid phases. Light Zn isotopes are usually more mobile in soil solution, while heavy Zn isotopes are more likely to be complexed (Caldelas et Weiss 2017, Zhang et al. 2018).

In a study conducted by Pokrovsky et al. (2005), the isotopic fractionation of Zn caused by adsorption on mineral surfaces such as birnessite, corundum, gibbsite, goethite, hematite, and pyrolusite did not exceed 0.2‰. The fractionation process during adsorption on mineral surfaces was presumably controlled by the fine structure of surface complexes and the position and bond strength for second neighbours of Zn.

Balistrieri et al. (2008) studied fractionation of Zn and Cu isotopes during adsorption onto amorphous ferric oxyhydroxide, namely, synthetic ferrihydrite, using comparatively pure river water and metal-rich acid rock drainage. Results indicate that the heavier isotope favourably adsorbs onto the surface of oxyhydroxide, which corresponds to shorter metal-oxygen bonds and a lower coordination number for the metal at the surface compared to the aqueous ion. The resulting fractionation was greater for Cu ($\Delta^{65/63}$Cu$_{\text{solution–solid}}$ = -0.73 ± 0.08‰) than for Zn ($\Delta^{66/64}$Zn$_{\text{solution–solid}}$

= -0.52 ± 0.04‰) because stronger metal binding occurs between the oxyhydroxide and Cu than with Zn.

Ferrihydrite was together with goethite also investigated in a study by Juillot et al. (2008). Like in the previous study, the solid's surface of Fe oxyhydroxides was also enriched with heavy isotopes. According to the authors, the fractionation appeared to proceed through an equilibrium mechanism. The different magnitudes of Zn fractionation between goethite ($\Delta^{66/64}Zn_{sorbed-aqueous}$ ≈ +0.29‰) and 2-lines ferrihydrite ($\Delta^{66/64}Zn_{sorbed-aqueous}$ ≈ +0.53‰) seemed to be related to structural differences between Zn complexes present on the surface of 2-lines ferrihydrite (tetrahedrally coordinated Zn), and goethite (octahedrally coordinated Zn).

In poorly crystalline Mn oxyhydroxide (birnessite) are the heavy isotopes also preferentially associated with the sorbent phase, as presented in the study by Bryan et al. (2015). At low ionic strength was observed an initial kinetic isotope fractionation effect with lighter isotopes adsorbed ($\Delta^{66/64}Zn_{adsorbed-dissolved}$ ≈ -0.2‰) which was then reduced to little or no isotope fractionation ($\Delta^{66/64}Zn_{adsorbed-dissolved}$ ≈ +0.05 ± 0.08‰) after 100 h when dissolved and birnessite-adsorbed Zn exchanged. By comparison, at high ionic strength, heavy Zn isotopes were preferentially adsorbed onto synthetic birnessite ($\Delta^{66/64}Zn_{adsorbed-dissolved}$ up to +2.7‰), reflecting equilibrium isotope fractionation.

Guinoiseau et al. (2016) were studying Zn isotope fractionation during sorption onto kaolinite. Heavy Zn isotopes were enriched on the surface of the mineral as well as in previously mentioned studies. $\Delta^{66/64}Zn_{adsorbed-solution}$ was ranging from 0.11‰ at low ionic strength and low pH to 0.49‰ at high ionic strength and high pH, which indicates that Zn isotope fractionation during sorption is mainly controlled by the chemical composition of the solution, such as pH or ionic strength.

Zn fractionation during adsorption onto organic matter was analysed using purified humic acid in a study by Jouvin et al. (2009). At pH above 6, Zn bound to purified humic acid was heavier than free Zn cations ($\Delta^{66}Zn_{purified\ humic\ acid\ -\ free\ Zn\ cations}$ = +0.24 ± 0.06‰). In contrast, at pH below 6, adsorption of Zn onto purified humic acid resulted in no measurable isotopic fractionation. That can be explained by changes in Zn speciation with pH, with higher complexation constants and shorter bond lengths for a complex of Zn and purified humic acid compared to the free Zn cations.
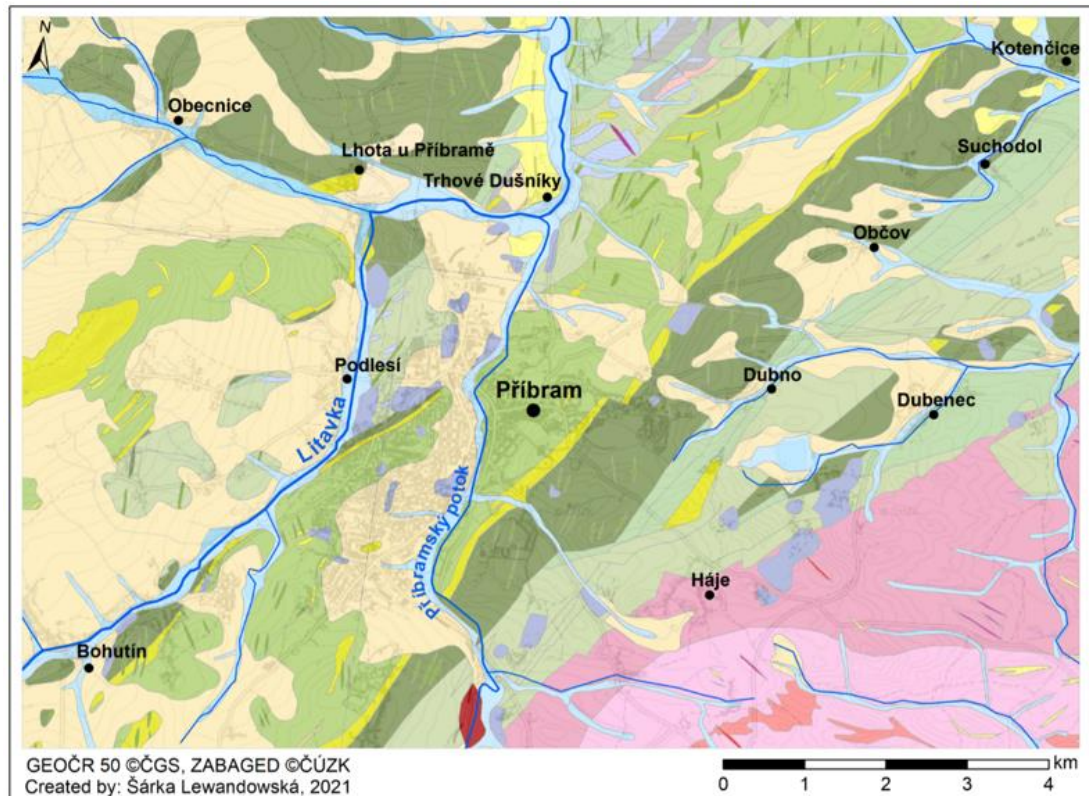
4. CHARACTERISTICS OF THE STUDY AREA

4.1   History of mining

Příbram is a town located in the Central Bohemian Region, about 60 km south-west to Prague, the capital of the Czech Republic. The town is situated on the eastern side of Brdy Highland in the valley of the Litavka river. Another stream flowing through the town is called Příbramský potok. The town and its surroundings have an increased load of pollution as a result of past mining activities (Nováková et al. 2015). The locality belongs to the Příbram ore region, which produced vein-type Ag, Pb, and Zn ores for centuries. The oldest written document about mining and smelting in Příbram dates back to the year 1311. During the Middle Ages, the former settlement became a small town, and the first Ag and Pb mines were established. In the 16th century, there was a significant development of Ag and Pb mines, and Příbram was promoted to a royal mining town by king Rudolf II. At the beginning of the 18th century, the mining of non-ferrous metal ores increased. At the end of the 19th century, Ag and Pb mines stagnated. However, after World War II, mining focused on newly discovered uraninite veins. U was mined here up until the 1990s. The total production of the whole district from the Medieval Period to the end of the 20th century was about 500 000 tons of Pb, 3 500 tons of Ag, and 49 990 tons of U (Glet 2018, Pánek et Hradecký 2016).

Although the mines are currently closed in this area, the smelter is still active. The smelter was established in 1786 because the old smelter was not able to process all the material coming from the newly opened mine in 1779. Since 1972 the smelter stopped processing primary ore material and continued with secondary material, such as lead-acid batteries. That included many problems because it was very difficult to find appropriate technology, and in the 1990s, the company Kovohutě Příbram was criticised for environmental reasons. However, new improved technologies were implemented in 1997, and the company is no longer a threat to the region (Dostál et al. 2006).

Geologically (Fig. 17), Příbram mining district creates a borderline between two geological regions of Bohemian Massif unit – Central Bohemian region (Bohemicum), made of Proterozoic and Cambrian folded sediments; and Moldanubicum, which is formed with granitoids of Middle Bohemian Pluton. Platform cover consists of Quaternary sediments. Moreover, this place lies on the crossing of two faults: Middle Bohemian deep fault and Jáchymov deep fault.

BOHEMICUM

Proterozoic: Neoproterozoic

- Greywacke, siltstone, shale
- Phyllitic black shale
- Basalt, basaltic andesite, tuff
- Trondhjemite

Paleozoic: Cambrian

- Basalt (diabase)
- Polymictic conglomerate
- Conglomerate
- Greywacke, arkose, sandstone
- Greywacke, arkose, siltstone, sandstone
- Clay shale

MOLDANUBICUM

Paleozoic: Carboniferous-Permian

- Fine-grained biotite granite with tourmaline
- Coarse-grained biotite granite with amphibole
- Granodiorite
- Basaltic andesite

PLATFORM

Cenozoic: Quarternary

- Slag heap
- River sediment
- Sand, gravel
- Silt, sand, gravel sediment
- Loess, loamy loess

Fig. 17: Geologic map of Příbram (ČGS ©2021, ČÚZK ©2021).

4.2 Sampling sites

A total of 5 sampling sites were selected for this study. The positions of sampling sites are shown in Fig. 18. Location 1 is situated at the university's research property located at Trhové Dušníky, which is a village about 4 km north-east to Příbram. This site is in the alluvium of the Litavka river. Location number 2 is a field, and number 3 is a forest area. Both locations are in the vicinity of alluvium. In addition, this place lies in the way of prevailing SW to NE wind blow direction containing emissions from a local smelter. Sampling sites 4 and 5 are adjacent to smelting works, site number 4 is a field, and number 5 is a forest.
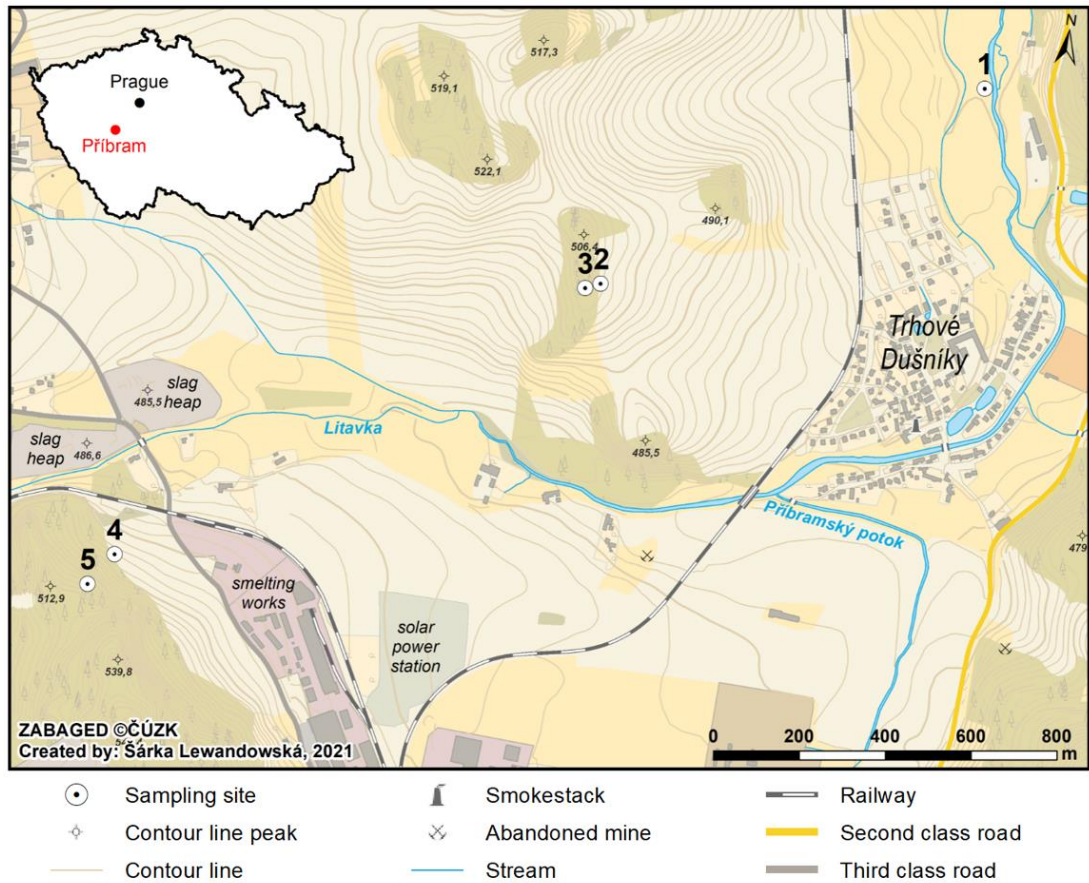
Fig. 18: Detailed map of the northern Příbram with marked sampling sites (ČÚZK ©2021).

5. Methodology

5.1   Soil samples characterisation and metal fractionation

The soil samples have been collected from the top soil layer (0-20 cm), air-dried, homogenised, and sieved through a 2-mm stainless sieve prior to subsequent laboratory analyses.

The active and exchangeable pH were determined in suspension with water or 1 M KCl (BS ISO 10390:2005). The content of organic/inorganic carbon (TOC/TIC) was determined using the carbon analyser TOC-L CPH (Shimadzu, Japan). The total content of metals was determined after digestion with 9 ml HNO_3 + 3 ml HCl + 3 ml HF under microwave conditions (Multiwave PRO, Anton Paar, Austria) (USEPA 3052). After the digestion, the remaining acids' mixture was evaporated from the sample and 2 ml of H_2O_2 were added and let to stay overnight. Next day, the H_2O_2 was evaporated (70 °C) and the sample was dissolved in 0.5 M HNO_3. The contents of metals in extracts were determined using inductively coupled plasma optical emission spectrometry (ICP-OES; iCAP 7000 series, Thermo Scientific, Germany), and trace metals concentrations were determined by inductively coupled plasma mass spectrometer (ICP-MS; iCAP Q, Thermo Scientific, Germany). Analytical quality control was conducted using certified reference material (NIST SRM 2711a, Soil Montana II).

Fractionation of metals in the soil was determined using different types of simple extractions. An exchangeable fraction has been isolated using a simple extraction with 0.5 M KNO_3 (1:5 w/v, 2 hours shaking). The acido-soluble fraction has been extracted using 1 M CH_3COONa buffered to pH 5 with acetic acid (1:5 w/v, 2 hours shaking) (Krishnamurti et al. 1995). The phytoavailable pool of the metals was determined using extraction with 0.005 M DTPA + 0.01 M $CaCl_2$ buffered at pH 5.3 (1:5 w/v, 2 hours shaking) (Quantin et al. 2008). The suspensions after the extractions were centrifuged (5000 rpm, 10 min) and filtered through a 0.45 µm syringe filter. The concentrations of extracted metals were determined using ICP-OES. All the extractions were performed in duplicate. The standard reference materials 2710a Montana Soil I (NIST, USA) and CRM 483 (Institute for Reference Materials and Measurements, EU) were used for quality assurance and quality control (QA/QC). All chemicals used were of analytical grade.

To access the readily mobile fraction of metals in soil, the diffuse gradients in thin film (DGT) devices were used (ZrO-Chelex- DGT Core, EasySensor, China). The samples

were proceeded according to the procedure provided by the manufacturer. The soil was watered to ~100% maximum water holding content. The watered soil was then filled inside the piston cavity and let to incubate for 24 hours in a plastic bag. Simultaneously, the portion of the same watered soil was put inside the oven to 60°C overnight to determine precisely the soil moisture content. After the 24 hours, the gel was carefully retrieved from the DGT probe and rinsed with the small amount of deionized water. Each gel disc was then put into the separate 2 ml tube and 1.8 ml of 1 M HNO_3 was added to elute the cations. The tubes were left to stand at room temperature for 16 h to extract the cations bound in the gel. The HNO_3 eluate was collected, and the gel was rinsed with 1.8 ml of deionized water for 2 h to remove residual acid. The gel disc was then immersed in a volume of 1.8 ml of the mixed solution containing 0.2 M NaOH and 0.5 M H_2O_2 (denoted as 0.2 M NaOH - 0.5 M H_2O_2) for 3-5 h to elute oxyanions bound on the gel (Wang Y. et al. 2017). The contents of Co, Ni, Cu, Zn, Cd, Pb, As, Sb, Se and V were determined using ICP-MS. The experiment DGT was performed in triplicate.

5.2   Isotopic measurements

5.2.1   Cd isotope measurements

Cd isotope ratios were measured using thermal ionization mass spectrometry (TIMS; Triton, Thermo Fisher), and Cd isotopic compositions are reported as $\delta^{114/110}Cd$, relative to the NIST SRM 3108, with Eq. 1:

$$\delta^{114/110}Cd = \left(\frac{\left(\frac{^{114}Cd}{^{110}Cd}\right)_{sample}}{\left(\frac{^{114}Cd}{^{110}Cd}\right)_{NIST\ SRM\ 3108}} - 1 \right) \times 1,000 \qquad (1)$$

Raw measurements were corrected for potential Cd isotope fractionation during the Cd purification procedure and the analysis, the double-spike (DS) method based on the nested iteration method was used. The DS was prepared by mixing two enriched Cd isotopes spikes: ^{106}Cd (97%) and ^{116}Cd (99%) purchased from IsoFlex, USA. The DS was added to the sample before the Cd separation process and was composed of ^{106}Cd (35%) and ^{116}Cd (65%). The natural/DS ratio was 5.6 for $^{106}Cd/^{110}Cd$ and 10.8 for $^{116}Cd/^{110}Cd$.

Before the Cd separation process, liquid samples were evaporated and directly transferred to bromide form. In contrast, bioavailability and acido-soluble solution were evaporated, dissolved in H_2O_2 to remove the organic compounds, and subsequently transferred to bromide form. Chromatographic separation of Cd was

performed following the analytical methods previously published (Schmitt et al. 2009a, Schmitt et al. 2009b, Abouchami et al. 2011, Abouchami et al. 2014). This technique was inspired by Pb separation and is promising because it is fast and requires only small amounts of acid. This protocol was adapted and recently applied in our laboratory at the Czech University of Life Sciences, using 400 µl of the BioRad AG1-X8 anion exchange resin (100-200 mesh) in bromide form (Table 6).

Tab. 6: Protocol for Cd purification by ion exchange chromatography (2 ml Column BioRad + 0.4 ml Resin AG1-X8 100-200 mesh).

Part		Reagent				
Order	Process	Step	Reagent	Volume	Time	Dose
Part I	Washing column	1	HNO_3 (0.5 M) normal pur	4 ml	2	2 ml
		2	H_2O Milli-Q	4 ml	2	2 ml
Part II	Conditioning	1	HNO_3 (0.5 M)-HBr (0.2 M) ultrapur	4 ml	4	1 ml
Part III	Sample Loading	1	HNO_3 (0.5 M)-HBr (0.2 M) ultrapur	2 ml	4	0.5 ml
Part IV	Matrix elution	1	HNO_3 (0.5 M)-HBr (0.2 M) ultrapur	2 ml	4	0.5 ml
		2	HNO_3 (0.45 M)-HBr (0.03 M) ultrapur	3 ml	3	1 ml
Part V	HBr Removing	1	HNO_3 (0.25 M) ultrapur	100 µl	1	100 µl
Part VI	Cd recovery	1	HNO_3 (0.25 M) ultrapur	6 ml	6	1 ml

After Cd recovery, the sample was evaporated entirely on a hot plate (110-120°C) to the last drop. After cooling, an activator was added to the sample depending on the amount of Cd. For 500 ng of Cd, the activator was composed of 50 µl of H_3PO_4 0.1 N and 100 µl of silica gel (100 mg/l of Si). The sample was then evaporated to dryness, and 10 µl of 2% HNO_3 was added and treated by ultrasonication. The volume was loaded stepwise onto outgassed single Re filaments. Additionally, to evaluate the Cd purification procedure and the analysis, the full purification procedure was applied for standard solutions (BAM-I012 and NIST SRM 3108) and international soil standard (NIST SRM 2711a Montana soil II). The samples were subsequently analysed using the TIMS.

5.2.2 Zn isotope measurements

Zn isotope ratios were measured using multicollector-inductively coupled plasma mass spectrometer (MC-ICP-MS; Neptune, Thermo Fisher) equipped with a desolvating nebulizer (Aridus II, Cetac) and Zn isotopic compositions are reported as $\delta^{66/64}Zn$, relative to the NIST SRM 683, proposed as new reference standard for Zn isotopes (Yang et al. 2018) with Eq. 2:

$$\delta^{66/64}Zn = \left(\frac{\left(\frac{^{66}Zn}{^{64}Zn}\right)_{sample}}{\left(\frac{^{66}Zn}{^{64}Zn}\right)_{NIST\ SRM\ 683}} - 1 \right) \times 1,000 \quad (2)$$

Zn for isotope analysis was separated from matrix solution by anion-exchange chromatography, using a modified procedure by Chapman et al. (2006) and Wombacher et al. (2003). The AG1-X8 resin (200-400 mesh, Bio-Rad) in chloride form was added to the column and was pre-conditioned with 6 ml of 6 M HCl. The Zn was separated from the samples using the procedure summarized in Table 7.

Tab. 7: Protocol for Zn purification by anion-exchange chromatography (10 ml Column BioRad + 2 ml Resin AG1-X8 200-400 mesh).

Part		Reagent			
Order	Process	Reagent	Volume	Time	Dose
Part I	Washing column	H_2O Milli-Q	20 ml	2	10 ml
Part II	Conditioning	HCl (6 M) ultrapur	6 ml	3	2 ml
Part III	Sample Loading	HCl (6 M) ultrapur	0.5 ml	1	0.5 ml
Part IV	Matrix elution	HCl (6 M) ultrapur	4 ml	4	1 ml
Part V	Cu elution	HCl (5 M) ultrapur	10 ml	10	1 ml
Part VI	Fe elution	HCl (1 M) ultrapur	10 ml	5	2 ml
Part VII	Zn recovery	HNO_3 (0.5 M) ultrapur	10 ml	5	2 ml

After the chemical separation, Zn eluate was evaporated to the last drop and 100 µl of concentrated HNO_3 were added to remove the traces of chlorides and nitrates. The latter step is repeated twice, and the dry residue is then dissolved in 5 ml of 2% HNO_3 for measurement. In the case of Zn isotope analysis, the MC-ICP-MS instrument was operated in the medium-resolution mode, and the masses 64, 66, 67, 68 and 70 were simultaneously detected. For the mass bias correction, the double spike method based on nested-iteration subtraction was applied. Double spike ^{67}Zn-^{70}Zn was prepared from two enriched Zn isotopes (Isoflex, USA).

6. RESULTS

6.1 Basic soil characterisation

The total content of selected potentially toxic elements (As, Cd, Cu, Pb, and Zn) is presented in Table 8. Based on the mean values (mg/kg), the order of abundance was following: Pb > Zn > As > Cu > Cd. Sampling site number 5 (forest near smelter) had the highest content of As (1 146 ± 82 mg/kg) and Pb (16 907 ± 1 963 mg/kg). On the contrary, the lowest concentration of both elements was found at site number 2 (field near alluvium), 20 ± 1 mg/kg of As and 280 ± 5 mg/kg of Pb. The concentration of Zn ranged from 79 ± 0 mg/kg in the sample from site number 3 (forest near alluvium) to 3 059 ± 148 mg/kg in the sample from locality 1 (alluvium). Cd concentrations ranged from 2 ± 0 mg/kg in samples 2 and 3 (field and forest near alluvium) to 29 ± 3 mg/kg in the sample from locality 1. The total levels of Cu ranged from 1 ± 1 mg/kg (sample 2) to 194 ± 30 mg/kg (sample 5, forest near smelter). Overall, the highest amount of contaminants was found in samples from locality 1 (alluvium) and 5 (forest near smelter).

Tab. 8: Concentrations of selected potentially toxic elements in the soil samples. The table depicts the average values and the corresponding standard deviations (n=2).

Sample	As	Cd	Cu	Pb	Zn
	mg.kg^{-1}				
1	220 ± 5	29 ± 3	51 ± 4	2 728 ± 283	3 059 ± 148
2	20 ± 1	2 ± 0	1 ± 1	280 ± 5	134 ± 5
3	41 ± 0	2 ± 0	16 ± 0	1 382 ± 38	79 ± 0
4	86 ± 4	6 ± 0	22 ± 3	1 472 ± 112	246 ± 18
5	1 146 ± 82	10 ± 1	194 ± 30	16 907 ± 1 963	307 ± 26

The soil samples' characterisation in terms of pH and carbon content is presented in Table 9. Overall, the pH was acidic (active pH ranging from 3.39 to 6.14). In addition, the forest samples (3 and 5) had significantly lower pH than others – for locality 3 was the active pH 3.39, and for locality 5 it was 3.65. The vast majority of total carbon (TC) was present in the form of organic carbon (OC). The highest content of inorganic carbon (IC) was found in the sample 2 collected on a field near alluvium (0.04 ± 0.04%). The organic carbon content for samples collected in alluvium and field (samples 1, 2, 4) ranged from 2.00 ± 0.07% to 2.55 ± 0.20%. This parameter was higher for forest soil samples, 6.25 ± 0.16% for sample 5 and even higher for sample 3 (17.52 ± 0.74%).

Tab. 9: Measured active (pH$_W$) and exchangeable (pH$_{KCl}$) pH and the carbon content in soil samples (mean value of the duplicates and standard deviation).

| Sample	pH$_w$	pH$_{KCl}$	TC	IC	OC
			wt%		
1	6.14	5.57	2.55 ± 0.20	0.02 ± 0.00	2.55 ± 0.20
2	6.12	5.53	2.13 ± 0.23	0.04 ± 0.04	2.13 ± 0.23
3	3.39	2.78	17.52 ± 0.74	0.01 ± 0.00	17.52 ± 0.74
4	4.94	4.26	2.00 ± 0.07	0.01 ± 0.00	2.00 ± 0.07
5	3.65	2.97	6.25 ± 0.16	0.01 ± 0.00	6.25 ± 0.16

6.2 Extraction procedures

The results obtained for selected potentially toxic elements after the application of four extraction procedures – DGT technique and single extractions with 1 M KNO$_3$, 1 M CH$_3$COONa, and mixture of 0.005 M DTPA with 0.01 M CaCl$_2$ (designated just as DTPA) – to the soil samples are reported in Table 10. The extractable percentage (% of [C]$_{tot}$) with respect to the trace element content in samples (from Tab. 8) is also given.

As shown, the extracted concentrations of As were below the limit of detection when KNO$_3$ was applied, and the maximal amount did not exceed 1.1% of its total concentration (sample 3 using DGT) when other extracting techniques were applied. In the case of Cu, the DTPA reagent was significantly more efficient for its extraction compared to other techniques. For example, in sample 1, the DTPA-extractable Cu concentration was 16.1 ± 0.7 mg/kg (31.5% of total), while CH$_3$COONa extracted 2.4 ± 0.0 mg/kg (4.7% of total), DGT 0.239 ± 0.005 mg/kg (0.5% of total) and the extracted concentration was below the limit of detection when KNO$_3$ was applied. The concentration of Pb extracted with CH$_3$COONa and DTPA was higher compared to KNO$_3$ and DGT technique. For example, in sample 4, CH$_3$COONa extracted 24.5% (360.2 ± 16.2 mg/kg) of total Pb (1 472 ± 112 mg/kg), DTPA extracted 50.2% (738.7 ± 10.1 mg/kg) of total Pb, while KNO$_3$ extracted 1.4% (20.4 ± 0.7 mg/kg) and DGT only 0.015% (216.2 ± 11.2 µg/kg) of total Pb. A similar leaching pattern (DTPA > CH$_3$COONa > KNO$_3$ > DGT) was also observed for other samples, except sample 5, where the highest amount of Pb was extracted using CH$_3$COONa (6 064.2 ± 189.1 mg/kg, 35.9% of total Pb).

As can be observed in Figure 19, for all the samples analysed, the concentration of Cd and Zn in the extracts followed the same sequence: DTPA > CH$_3$COONa > KNO$_3$ > DGT. The highest portion of Cd was extracted after application of DTPA – up to 84.7% (2.1 ± 0.0 mg/kg) of total Cd content in sample 3. In general, about 50% of Cd was extracted, while for Zn it was about 10% to 30%, indicating that Cd is relatively

more mobile than Zn. The DGT-extractable Cd ranged from 25.5 ± 2.3 µg/kg (sample 2, 1.0% of total) to 146.6 ± 3.5 µg/kg (sample 1, 0.5% of total) and Zn ranged from 69.9 ± 11.0 µg/kg (sample 2, 0.1% of total) to 11 461.2 ± 47.0 µg/kg (sample 1, 0.4% of total). For both Cd and Zn, the extracted concentrations were below the detection limit for soil sample 2 when KNO_3 was applied. The differences in performance between single extracting agents were least significant in sample 5, in which they all extracted about 22% of total Cd and 11% of total Zn present in the soil.
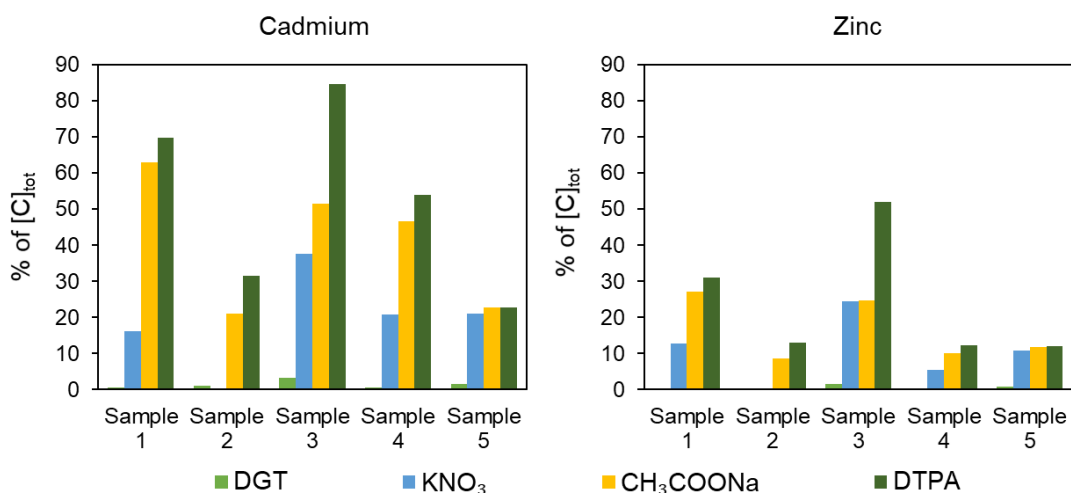
Fig. 19: Extracted amount (% of total concentration) of Cd (left) and Zn (right) from samples 1 to 5 using various extracting techniques (DGT, KNO_3, CH_3COONa, DTPA with $CaCl_2$).

The metal extraction efficiency obtained with the four studied extracting procedures can be compared by observing the results depicted in Figures 20 and 21. In general, the highest extraction efficiency was obtained with DTPA, followed by CH_3COONa. On the contrary, the lowest extraction efficiency was generally obtained with the DGT technique, which suggests that it was able to extract just the most mobile fraction of targeted metal(loid)s. Extractability performance of KNO_3 towards some elements (e.g., As and Cu) was rather low.

According to the extracted portion from the total content of elements present in the samples, the order of mobility using DGT technique was following: Cu > Cd > Zn > As > Pb, indicating that although the Pb was present in samples in high concentrations, only a relatively small portion was mobile and available to plants. However, the CH_3COONa and DTPA reagents were able to extract comparatively higher percentage of Pb with the respect to its total content in samples (up to 81% of total Pb), thereby classifying Pb among more mobile elements. The least mobile element regarding extracted portion after the application of single extractants was always As and the most mobile element was always Cd.
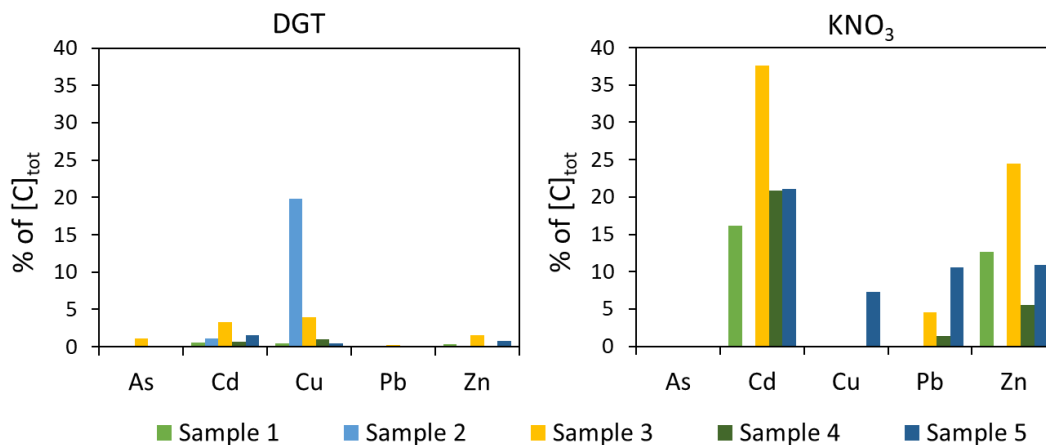
Fig. 20: Comparison of extractability of various potentially toxic elements in samples using different extracting procedures (DGT on the left, KNO₃ on the right).
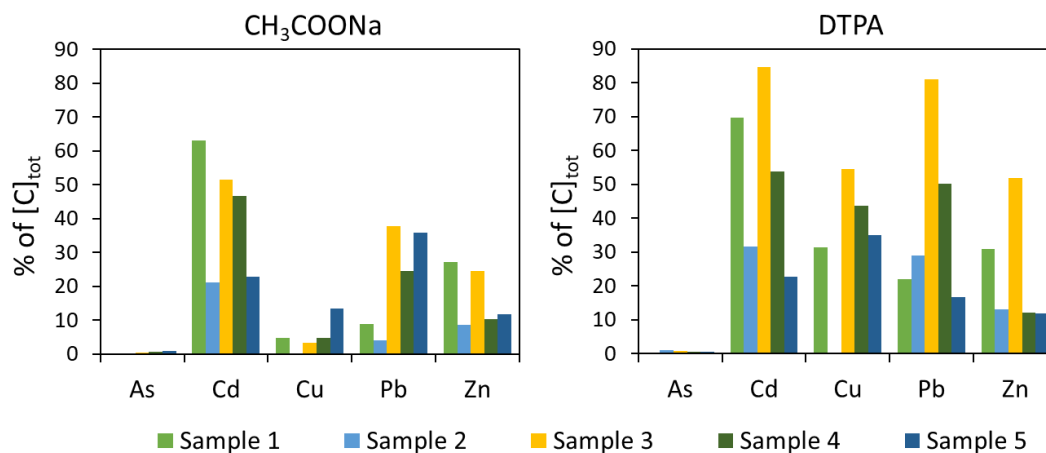
Fig. 21: Comparison of extractability of various potentially toxic elements in samples using different extracting procedures (CH₃COONa on the left, DTPA with CaCl₂ on the right).

Tab. 10: Extractable concentrations (mean ± SD (n=2 for single extractants; n=3 for DGT)) of selected potentially toxic elements in soil samples after applying three single extraction procedures (with extracting agents KNO$_3$, CH$_3$COONa, DTPA with CaCl$_2$) and DGT technique; BDL stands for below detection limit.

Sample	Extracting method	Units	As	Cd	Cu	Pb	Zn
1	DGT	µg/kg	10.0 ± 2.0	146.6 ± 3.5	239.7 ± 5.4	77.0 ± 17.8	11 461.2 ± 47.0
		% of [C]$_{tot}$	0.0	0.5	0.5	0.0	0.4
	KNO$_3$	mg/kg	BDL	4.6 ± 0.1	BDL	2.7 ± 0.1	387.0 ± 28.3
		% of [C]$_{tot}$	-	16.2	-	0.1	12.7
	CH$_3$COONa	mg/kg	BDL	18.0 ± 0.3	2.4 ± 0.0	242.1 ± 4.3	829.1 ± 13.7
		% of [C]$_{tot}$	-	63.1	4.7	8.9	27.1
	DTPA	mg/kg	BDL	19.9 ± 0.6	16.1 ± 0.7	599.0 ± 11.8	948.2 ± 28.1
		% of [C]$_{tot}$	-	69.7	31.5	22.0	31.0
2	DGT	µg/kg	23.4 ± 1.4	25.5 ± 2.3	194.5 ± 4.0	20.0 ± 4.6	69.9 ± 11.0
		% of [C]$_{tot}$	0.1	1.0	19.8	0.0	0.1
	KNO$_3$	mg/kg	BDL	BDL	BDL	BDL	BDL
		% of [C]$_{tot}$	-	-	-	-	-
	CH$_3$COONa	mg/kg	BDL	0.5 ± 0.0	BDL	11.4 ± 0.0	11.4 ± 0.3
		% of [C]$_{tot}$	-	21.1	-	4.1	8.5
	DTPA	mg/kg	0.2 ± 0.0	0.8 ± 0.0	2.1 ± 0.1	81.0 ± 1.4	17.4 ± 0.4
		% of [C]$_{tot}$	1.0	31.6	216.8	28.9	13.0
3	DGT	µg/kg	460.9 ± 51.4	82.5 ± 1.8	629.1 ± 44.6	3 539.6 ± 53.5	1 207.7 ± 96.1
		% of [C]$_{tot}$	1.1	3.3	3.9	0.3	1.5
	KNO$_3$	mg/kg	BDL	0.9 ± 0.0	BDL	62.6 ± 0.2	19.2 ± 0.3
		% of [C]$_{tot}$	-	37.6	-	4.5	24.5
	CH$_3$COONa	mg/kg	0.1 ± 0.0	1.3 ± 0.0	0.5 ± 0.1	522.4 ± 3.3	19.3 ± 0.4
		% of [C]$_{tot}$	0.3	51.4	3.3	37.8	24.6
	DTPA	mg/kg	0.3 ± 0.2	2.1 ± 0.0	8.7 ± 0.1	1 119.7 ± 3.0	40.8 ± 0.4
		% of [C]$_{tot}$	0.7	84.7	54.4	81.0	51.9
4	DGT	µg/kg	119.5 ± 3.5	38.3 ± 1.0	202.9 ± 26.5	216.2 ± 11.2	224.8 ± 3.2
		% of [C]$_{tot}$	0.1	0.6	0.9	0.0	0.1
	KNO$_3$	mg/kg	BDL	1.2 ± 0.0	BDL	20.4 ± 0.7	13.5 ± 0.3
		% of [C]$_{tot}$	-	20.9	-	1.4	5.5
	CH$_3$COONa	mg/kg	0.6 ± 0.7	2.8 ± 0.1	1.0 ± 0.2	360.2 ± 16.2	25.1 ± 0.7
		% of [C]$_{tot}$	0.7	46.7	4.7	24.5	10.2
	DTPA	mg/kg	0.5 ± 0.0	3.2 ± 0.1	9.5 ± 0.2	738.7 ± 10.1	29.9 ± 0.8
		% of [C]$_{tot}$	0.6	53.9	43.6	50.2	12.2
5	DGT	µg/kg	685.9 ± 58.2	142.8 ± 14.6	732.3 ± 63.6	20 217.2 ± 2 045.3	2 324.3 ± 194.6
		% of [C]$_{tot}$	0.1	1.5	0.4	0.1	0.8
	KNO$_3$	mg/kg	BDL	2.0 ± 0.0	14.1 ± 0.2	1 782.4 ± 17.1	33.5 ± 0.1
		% of [C]$_{tot}$	-	21.0	7.3	10.5	10.9
	CH$_3$COONa	mg/kg	10.1 ± 4.5	2.2 ± 0.1	26.0 ± 1.3	6 064.2 ± 189.1	35.9 ± 2.7
		% of [C]$_{tot}$	0.9	22.8	13.4	35.9	11.7
	DTPA	mg/kg	5.3 ± 0.2	2.2 ± 0.1	67.8 ± 1.4	2 811.3 ± 19.6	36.8 ± 1.0
		% of [C]$_{tot}$	0.5	22.7	34.9	16.6	12.0

6.3 Isotopic fractionation of Cd and Zn

The observed $\delta^{114/110}Cd$ and $\delta^{66/64}Zn$ values gained from the soil samples (TOTAL) and solution after extraction with different extracting procedures (DGT, KNO_3, CH_3COONa, DTPA with $CaCl_2$ – designated as DTPA) are listed in Table 11. Graphs depicting the variation of delta values of Cd and Zn in samples 1 to 5 are showed in Figures 22 to 26. Since the concentration of Cd in sample 2 was too low (Tab. 8), it was not possible to measure Cd isotopes at all (N/A). Moreover, there were some technical difficulties with several measurements of Cd isotopes in samples 3 and 5 and sample 2 for Zn during the time of thesis writing. For this reason, these data could not be included in the thesis.

Tab. 11: Delta values ($\delta^{114/110}Cd$ and $\delta^{66/64}Zn$) of the soil samples (TOTAL) and soil solution after extraction with three single extraction procedures (with extracting agents KNO_3, CH_3COONa, DTPA with $CaCl_2$) and DGT technique; N/A stands for not analysed. The values are represented in the mean values and the standard deviations (for Cd) or standard error (for Zn).

| Sample	Type	$\delta^{114/110}Cd$	2SD	$\delta^{66/64}Zn$	2SE
		‰			
1	TOTAL	-0.34	0.03	-0.09	0.00
	DGT	-0.30	0.01	-0.16	0.01
	KNO_3	-0.16	0.03	0.02	0.00
	CH_3COONa	-0.31	0.01	0.03	0.01
	DTPA	-0.34	0.07	0.00	0.01
2	TOTAL			-0.13	0.01
	DGT			-0.12	0.01
	KNO_3	N/A		N/A	
	CH_3COONa			-0.57	0.00
	DTPA			0.04	0.01
3	TOTAL	N/A		-0.18	0.01
	DGT	-0.18	0.13	-0.33	0.01
	KNO_3	-0.12	0.06	-0.17	0.01
	CH_3COONa	-0.16	0.12	-0.28	0.02
	DTPA	-0.22	0.04	-0.34	0.02
4	TOTAL	-0.24	0.05	-0.20	0.01
	DGT	0.07	0.02	-0.29	0.01
	KNO_3	0.11	0.06	0.03	0.01
	CH_3COONa	-0.02	0.01	-0.06	0.01
	DTPA	0.01	0.04	-0.07	0.01
5	TOTAL	N/A		-0.22	0.03
	DGT	-0.35	0.11	-0.40	0.02
	KNO_3	N/A		-0.48	0.00
	CH_3COONa	N/A		-0.33	0.01
	DTPA	-0.25	0.01	-0.39	0.00

As shown, the original soil samples (TOTAL) were depleted in heavy Cd isotopes compared to the standard, $\delta^{114/110}Cd$ = -0.34 ± 0.03‰ in sample 1 and $\delta^{114/110}Cd$ = -0.24 ± 0.05‰ in sample 4. The soil samples were also depleted in heavy Zn isotopes relative to the standard, $\delta^{66/64}Zn$ values ranging from -0.09 ± 0.00‰ in sample 1 to -0.22 ± 0.03‰ in sample 5.

Comparing the isotopic composition of soil with extracted solutions, the DTPA extract in sample 1 had the same $\delta^{114/110}Cd$ value (-0.34 ± 0.07‰) as total soil (-0.34 ± 0.03‰). Otherwise, all extracts of samples 1 and 4 were enriched in heavy Cd isotopes compared to the soil. For example, in sample 4, the $\delta^{114/110}Cd$ value of soil was -0.24 ± 0.05‰, whereas the Cd isotopes in the extracts were heavier than those in the bulk soil, $\delta^{114/110}Cd$ values ranging from -0.02 ± 0.01‰ (CH_3COONa) to 0.11 ± 0.06‰ (KNO_3). That suggests that heavier Cd isotopes are preferentially partitioned into the soil solution, thereby being exchangeable and available to plants. Besides that, the extracts after application of KNO_3 showed the highest enrichment of heavy Cd isotopes compared to other extracting techniques, for example in sample 3, $\delta^{114/110}Cd$ values of solution after KNO_3 extraction was -0.12 ± 0.06‰, while other $\delta^{114/110}Cd$ values were -0.18 ± 0.13‰ for DGT, -0.16 ± 0.12‰ for CH_3COONa and -0.22 ± 0.04‰ for DTPA. On the contrary, either DGT or DTPA measurements were usually depleted in heavy Cd isotopes the most among other extracting procedures.

Analysis of Zn isotopes revealed that the DGT measurements were more depleted in heavy Zn isotopes compared to the soil, except for sample 2, where both $\delta^{66/64}Zn$ values were similar (-0.13 ± 0.01‰ for soil and -0.12 ± 0.01‰ for DGT extract). In samples 3 and 5 (forest samples), the solutions after single extractions were also mostly more depleted in heavy isotopes relative to soil, except for KNO_3 measurement in sample 3 ($\delta^{66/64}Zn$ = -0.17 ± 0.01‰), which was slightly less isotopically depleted than soil ($\delta^{66/64}Zn$ = -0.18 ± 0.01‰). In contrast, all solutions after single extractions in samples 1 and 4 were enriched in heavy isotopes compared to the soil. For example, in sample 4, the $\delta^{66/64}Zn$ values in solution after application of all three single extractants ranged from -0.07 ± 0.01‰ (DTPA) to 0.03 ± 0.01‰ (KNO_3), whereas the $\delta^{66/64}Zn$ value of soil was -0.20 ± 0.01‰.
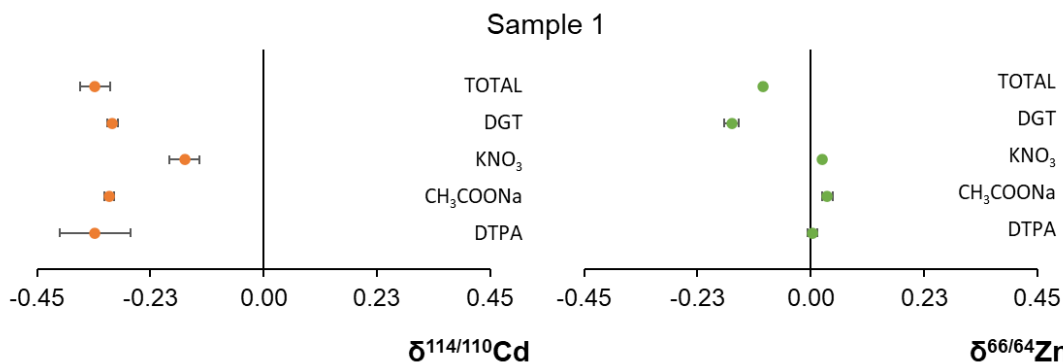
Fig. 22: Delta values of Cd (left) and Zn (right) in the soil (TOTAL) and soil solution (DGT, KNO₃, CH₃COONa, and DTPA with CaCl₂ extract) in sample 1.
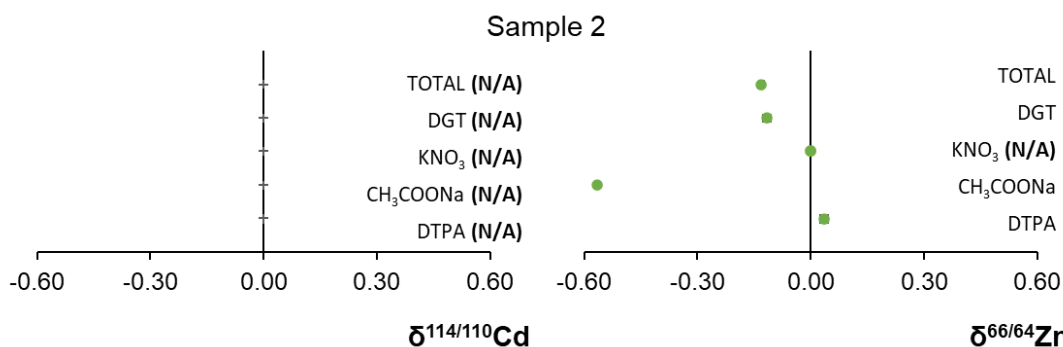
Fig. 23: Delta values of Cd (left) and Zn (right) in the soil (TOTAL) and soil solution (DGT, KNO₃, CH₃COONa, and DTPA with CaCl₂ extract) in sample 2; N/A stands for not analysed.
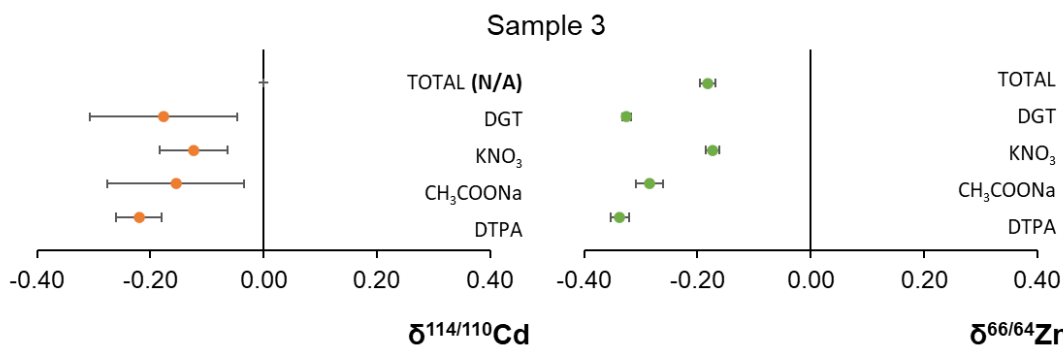
Fig. 24: Delta values of Cd (left) and Zn (right) in the soil (TOTAL) and soil solution (DGT, KNO₃, CH₃COONa, and DTPA with CaCl₂ extract) in sample 3; N/A stands for not analysed.

Fig. 25: Delta values of Cd (left) and Zn (right) in the soil (TOTAL) and soil solution (DGT, KNO₃, CH₃COONa, and DTPA with CaCl₂ extract) in sample 4.

45
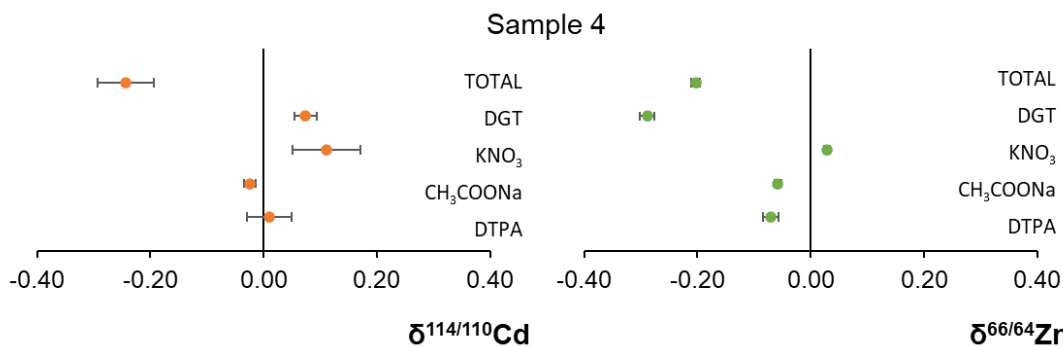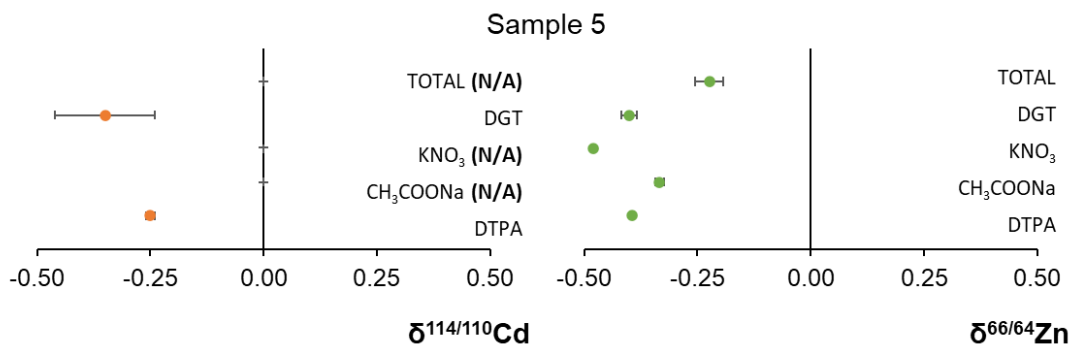
Fig. 26: Delta values of Cd (left) and Zn (right) in the soil (TOTAL) and soil solution (DGT, KNO₃, CH₃COONa, and DTPA with CaCl₂ extract) in sample 5; N/A stands for not analysed.

7. DISCUSSION

7.1   Basic soil characterisation

The limit values set for metals and metalloids in agricultural soils by the Ministry of the Environment of the Czech Republic in Decree No. 153/2016 Coll. were exceeded in most of the studied soil samples (see Tab. 12). The levels of As, Cd and Pb were surpassed in all samples. Even though sample number 2 (collected on crop field) had the lowest concentrations of selected elements relative to other sampling sites, this locality is still clearly not suitable for agricultural activity. The limit values of Cd were exceeded 4x, Pb limits were surpassed almost 5x, and the concentrations of As and Zn also reached the limit values. In contrast, concentrations of some metal(loid)s in samples 1 and 5 were exceeded to an extreme degree (e.g., Zn in sample 1 more than 25x and Pb in sample 5 more than 250x).

Tab. 12: Limit and total (mean ± SD (n=2)) concentrations of selected elements in soil samples (all units are in mg.kg^{-1}).

Element	Limit	Sample				
		1	2	3	4	5
As	20	220 ± 5	20 ± 1	41 ± 0	86 ± 4	1 146 ± 82
Cd	0.5	29 ± 3	2 ± 0	2 ± 0	6 ± 0	10 ± 1
Cu	60	51 ± 4	1 ± 1	16 ± 0	22 ± 3	194 ± 30
Pb	60	2 728 ± 283	280 ± 5	1 382 ± 38	1 472 ± 112	16 907 ± 1 963
Zn	120	3 059 ± 148	134 ± 5	79 ± 0	246 ± 18	307 ± 26

Forest samples (3 and 5) presented to be more polluted than agricultural soil samples (2 and 4), possibly due to long-time pollutant deposition with less disturbance in forest area compared to the areas with agricultural activity. Also, in localities affected by smelting activity, the soils from forested areas tend to have higher metal and metalloid burdens than soils from the uncovered areas (e.g., crop fields or grasslands) due to retention of atmospheric particles and greater canopy interception (Palmer et al. 2021). In a study by Ettler et al. (2005), the authors also found notable differences in lead concentration between the forest and tilled soil samples collected in Příbram region, where the Pb concentrations in tilled soils were lower by one order of magnitude compared to forest soils. Authors reported that this difference could also be related to the annual harvesting of crops from the tilled soils.

The content of organic carbon in the Czech Republic ranges from 1.5 to 7% (on average 2-3%) in agricultural soils (Jeřábková 2019) and is higher for forest soils, for which is the mean content 23.5% (Gholizadeh et al. 2021). Therefore, the organic carbon in studied samples was normal for samples 1, 2, 4 and slightly lower for forest

samples (3, 5). Correspondingly, the pH was lower in forest samples. Naturally, forest soils tend to be more acidic than other soil types (e.g., agricultural soils) because the organic matter and minerals break down and degrade over time to more acidic substances (e.g., fulvic acids) lowering the soil pH (Sootahar et al. 2019). According to the indicators of quality of agricultural and forest soils in the Czech Republic published by the Ministry of the Environment of the Czech Republic, the pH of samples 1 and 2 was slightly acidic, samples 4 and 5 were strongly acidic, and sample 3 was extremely acidic (Sáňka et Materna 2004).

7.2   Extraction procedures

DGT technique is often regarded as a more robust tool compared to other traditional single-step extraction methods when predicting and assessing metal bioavailability in soils (Soriano-Disla et al. 2009, Wang P. et al. 2017). In a study by Dai et al. (2017), authors compared the DGT technique with several traditional extracting techniques (e.g., ethylene diamine tetraacetic acid (EDTA), acetic acid (CH_3COOH), calcium chloride ($CaCl_2$)) to evaluate Cd bioavailability in soil. For the DGT technique, the correlations between plant and soil Cd concentrations were independent of the soil properties (pH and organic carbon content) hence less influenced by them compared to traditional techniques. Moreover, a higher correlation coefficient compared to conventional techniques was achieved.

Extraction with KNO_3 is frequently performed as a first step in sequential extraction procedure. The metals extracted by KNO_3 are assumed to represent the most labile metal pool because the readily soluble form of trace metal is often regarded as the most bioavailable form (Prasad et al. 2006). Hence, the low amount of trace elements (As, Cu, Pb) in the extracted solution after application of this reagent in this study can indicate a low availability of these elements to plants.

CH_3COONa extraction is useful for predicting the available pool of trace elements adsorbed to the carbonates bound fraction of soils and sediments. DTPA is suitable to predict and quantify the exchangeable pools associated with organic matter and hydroxides (Coelho et al. 2018). The DTPA extraction repeatedly performs higher extractability of elements in a single extraction compared to the other extractants (e.g., Marchi et al. 2009, Qasim et al. 2015). Agbenin et al. (1999) suggested that the high extraction capacity of DTPA for some metals, such as Zn or Cu, might be ascribed to its two donor groups – the carboxylate (−COO−) and amine (−NH_2) group, which have considerable ability to complex metals.

Regarding the mobility of metals, Cd is often reported as the most mobile element (e.g., Devi et Bhattacharyya 2018, Król et al. 2020). Zn is also considered as a highly mobile element (Pueyo et al. 2004, Zalewska 2012). On the contrary, Pb is commonly referred to as an element with very low mobility (Vaněk et al. 2011). Cu and As have also been reported as low mobility elements (Vöröš et al. 2015). Vicente-Martorell et al. 2009 established the following ranking of metal bioavailability in sediments: Cd > Zn > Cu > Pb. In the experiment presented by this thesis, Cd and Zn were among the most mobile elements and Cu and As among the least mobile elements.

Soil pH is acknowledged as one of the most important factors determining not only the concentration of metals in the soil solution but also their mobility and availability to plants. The increase of hydrogen ion activity affects the mobilisation intensity of metals. In highly acidic soils, the mobility of metallic elements is much higher than in neutral or alkaline soils (Fijałkowski et al. 2012). Increased mobility in extremely acidic conditions (sample 3) was also observed in this study (Fig. 21), and it was especially noticeable when DTPA with $CaCl_2$ was applied.

7.3 Isotopic fractionation of Cd and Zn

Generally, the soils demonstrate depletion in heavy Cd isotopes with respect to the standard (NIST SRM 3108). Wang et al. (2019) presented that agricultural soils in China presumably supplied with Cd by ore smelting and/or refining processes had isotope compositions ($\delta^{114/110}Cd$) ranging from -0.76‰ to -0.25‰. Imseng et al. (2018) reported that Cd in soil ($\delta^{114/110}Cd$ = -0.21 to 0.14‰) was isotopically lighter than in plant harvest ($\delta^{114/110}Cd$ = 0.27 to 0.94‰). They also observed that soil-plant cycling extracted isotopically heavy Cd from the subsoil and relocated it to the topsoil.

Biological activity leads to preferential enrichment of either lighter or heavier Cd isotopes, possibly due to diverse strategies of plants to cope with Cd (Wang et al. 2021). For example, the majority of soils (with $\delta^{114/110}Cd$ of about -0.1‰ to 0‰.) from organic farms in Ecuador were isotopically lighter than the leaves and pods of cacao plants, with $\Delta^{114/110}Cd_{leaf-soil}$ values of 0.22 ± 0.07‰ to 0.41 ± 0.09‰ (Barraza et al. 2019). In contrast, Wei et al. (2018) observed systematic enrichment in light isotopes relative to the solutions for Cd tolerant plant *Ricinus communis* ($\Delta^{114/110}Cd_{plant-solution}$ = -0.64‰ to -0.29‰).

Results in the study by Zhang et al. (2021) suggest that heavier Cd is preferentially partitioned into the soil solution, being exchangeable and available to plant roots. Cd isotopes in 0.1 M $CaCl_2$ extract were significantly heavier compared to the bulk soil ($\Delta^{114/110}Cd_{extract-soil}$ = 0.42‰) in their study. Wiggenhauser et al. (2016) determined

isotope ratio in soil bulk and extractable Cd soil pool. Calcium nitrate ($Ca(NO_3)_2$) extractable Cd was isotopically heavier than the Cd in the soil bulk ($\Delta^{114/110}Cd_{extract-bulk}$ = 0.16 to 0.45‰).

The Zn isotopic composition in soils can be naturally very diverse, depending mainly on parent rock and anthropogenic activities. Igneous and sedimentary rocks show limited variations in their isotopic compositions ($\delta^{66/64}Zn$ = -0.22 to 0.28‰) excluding carbonates, which can be more enriched in heavy isotopes ($\delta^{66/64}Zn$ = 0 to 1.13‰). Anthropogenic activities cause larger isotopic variability ($\delta^{66/64}Zn$ = -0.98 to 0.53‰) primarily due to the evaporation and condensation processes of elemental Zn in metal refineries. Specific isotope composition of geogenic and anthropogenic sources can be used to trace Zn soil contamination sources (Imseng et al. 2019). During the investigation of soil contaminated by smelting processes, Bigalke et al. (2010) found out that the $\delta^{66/64}Zn$ values were isotopically lighter in ash (-0.41‰) and organic horizons (-0.85‰ to -0.47‰) than in bedrock (-0.28‰) and slag (0.18‰). This fractionation pattern was probably caused by the kinetic fractionation during evaporation, which subsequently allowed to distinguish between native Zn in soils and Zn that originated in smelter.

Besides diverse sources, biogeochemical processes can also generate significant Zn isotope fractionation in soils and plants. Heavy Zn isotopes are typically enriched in the root system of plants compared to the leaves, shoots and the host soil. (Fujii et Albarède 2012). Křibek et al. (2020) disclosed that the extent of biogenic Zn fractionation is strongly dependent on the plant-available concentration of Zn in soil. In their study, when the plant-available concentration of Zn was low (<20 mg/kg), the sap and leaves of birch were enriched with heavy isotopes (mean $\Delta^{66}Zn_{sap-substrate}$ = +0.45‰ and $\Delta^{66}Zn_{leaf-substrate}$ = +0.04‰). On the contrary, when the plant-available concentration of Zn was high (>20 mg/kg), the sap and leaves were depleted in heavy isotopes (mean $\Delta^{66}Zn_{sap-substrate}$ = -1.31‰ and $\Delta^{66}Zn_{leaf-substrate}$ = -0.93‰). Arnold et al. (2015) observed following fractionation between the total above-ground plant biomass and the soil leach after application of 0.1 M hydrochloric acid (HCl): $\Delta^{66/64}Zn_{plant\ above\ ground–soil\ leach}$ = -0.27 ± 0.09‰ in anaerobic and -0.08 ± 0.04‰ in aerobic soils. Authors anticipate that the secretion of root exudates (phytosiderophores), which probably accounts for higher Zn capture and incorporation of heavier isotopes due the complexation processes, is more evident in aerobic soils.

8. Conclusion and contribution of the thesis

The investigation of mobility of potentially toxic elements can be a suitable way to understand and evaluate the potential risks for the ecosystems in contaminated environment due to the possibility of subsequent plant uptake and biomagnification through a food chain. The isotopic data can provide an insight into the biogeochemical cycling of metals.

Total content, extraction and isotope analyses were carried out on soil samples collected in the Příbram region, known for historical mining, processing, and smelting of polymetallic ores resulting in metal pollution of surrounding soils and streams. The soil samples were classified as slightly to extremely acidic. The total concentrations of five elements, namely As, Cd, Cu, Pb, and Zn were determined. Based on the mean values (mg/kg), the order of abundance was as follows: Pb > Zn > As > Cu > Cd. Most of the metals in the study area exceeded the limits set for agricultural soils (Decree No. 153/2016 Coll.), some of them to an extreme extent, e.g., Pb more than 250x (16 907 ± 1 963 mg/kg), indicating possible ecological or health risks.

Concerning the effectivity of selected extracting procedures – DGT technique and single extractions with 1 M KNO_3, 1 M CH_3COONa, and mix of 0.005 M DTPA with 0.01 M $CaCl_2$ – relatively the biggest portion of targeted metals was extracted using DTPA with $CaCl_2$. On the contrary, the DGT technique was able to extract only the most mobile metal pool. Besides that, in the single extractions, Pb was represented as a relatively mobile element, while the DGT barely extracted any amount of Pb, suggesting considerably low mobility of this metal.

Isotopic data disclosed that the soil samples were depleted in heavy Cd and Zn isotopes relative to standards. The Cd isotopes in the extracts were heavier than those in the bulk soil, suggesting that heavier Cd isotopes are favourably partitioned into the soil solution, hence being exchangeable and available to plants. A similar trend was observed for Zn isotopes. However, the opposite trend was detected in forest samples, where the extracts were more depleted in heavy Zn isotopes compared to the bulk soil.

The obtained results are currently in preparation for submission to the *Journal of Hazardous Materials:*

Ratié G., Vaňková Z., Baragaño D., Liao R., Šípková A., Chrastný V., Lewandowská Š., Ding S., Gallego J. L. R., Komárek M., 2021: Insights of Cd and Zn isotope systematics in the available and remobilized fractions after industrial wastes deposition.

9. BIBLIOGRAPHY AND SOURCES USED

Scientific books:

AELION C. M., Höhener P., Hunkeler D., Aravena R. [eds.], 2010: Environmental Isotopes in Biodegradation and Bioremediation. CRC Press, Boca Raton.

AKASH M. S. H. et Rehman K., 2020: Essentials of Pharmaceutical Analysis. Springer Nature, Singapore.

ALEXANDRE P., 2020: Isotopes and the Natural Environment. Springer, New York.

ASRARI E., 2014: Heavy Metal Contamination of Water and Soil: Analysis, Assessment, and Remediation Strategies. Apple Academic Press, New York.

BINI C., 2010: From Soil Contamination to Land Restoration. Nova Science Publishers, Inc., New York.

BISEN P. S. et Sharma A., 2012: Introduction to Instrumentation in Life Sciences. CRC Press, Boca Raton.

CBCSS: Committee on Bioavailability of Contaminants in Soils and Sediments, 2003: Bioavailability of Contaminants in Soils and Sediments. The National Academies Press, Washington, D.C.

COBB A., 2008: Cadmium. Marshall Cavendish Benchmark, New Yok.

DAVISON W. [ed.], 2016: Diffusive Gradients in Thin-Films for Environmental Measurements. Cambridge University Press, Cambridge.

DOSTÁL J., Kunický Z., Vurm K., 2006: 220 let olověné a stříbrné hutě Příbram 1786-2006. Kovohutě Příbram, Příbram.

DOWNARD K., 2004: Mass Spectrometry: A Foundation Course. Royal Society of Chemistry, Cambridge.

EKMAN R., Silberring J., Westman-Brinkmalm A., Kraj A. [eds.], 2008: Mass Spectrometry: Instrumentation, Interpretation, and Applications. John Wiley & Sons, Inc., Hoboken.

ELLAM R., 2016: Isotopes: A Very Short Introduction. Oxford University Press, Oxford.

ENGHAG P., 2004: Encyclopedia of the Elements: Technical Data - History - Processing - Applications. John Wiley & Sons, Inc., Hoboken.

FARMER A., 1997: Managing Environmental Pollution. Routledge, Abingdon.

FRY B., 2007: Stable Isotope Ecology. Springer Science & Business Media, New York.

GAT J. R., 2010: Isotope Hydrology: A Study of the Water Cycle. Imperial College Press, London.

GLET J., 2018: Co možná nevíte o Středočeském kraji. KKnihy.cz, České Budějovice.

GRAY L., 2006: Zinc. Marshall Cavendish Benchmark, New Yok.

HESTER R. E. et Harrison R. M. [eds.], 2008: Environmental Forensics. Royal Society of Chemistry, Cambridge.

HOEFS J., 2015: Stable Isotope Geochemistry. Springer, New York.

HOEFS J., 2018: Stable Isotope Geochemistry. Springer International Publishing, Cham.

HOLMAN J. S. et Stone P., 2001: Chemistry. Nelson Thornes, Cheltenham.

HOODA P. S. [ed.], 2010: Trace elements in Soils. John Wiley & Sons, Ltd., Chichester.

JOHNSON A. et Singhal N., 2010: Amendment-Enhanced Phytoextraction of Soil Contaminants. Nova Science Publishers, Inc., New York.

KABATA-PENDIAS A. et Szteke B., 2015: Trace Elements in Abiotic and Biotic Environments. CRC Press, Boca Raton.

KABATA-PENDIAS A., 2010: Trace Elements in Soils and Plants. CRC Press, Boca Raton.

KARPAS Z., 2015: Analytical Chemistry of Uranium: Environmental, Forensic, Nuclear, and Toxicological Applications. CRC Press, Boca Raton.

KIRKLAND K., 2007: Particles and the Universe. Infobase Publishing, New York.

KONYA J. et Nagy N. M., 2012: Nuclear and Radiochemistry. Elsevier, London.

KREBS R. E., 2006: The History and Use of Our Earth's Chemical Elements: A Reference Guide. Greenwood Publishing Group, Inc., Westport.

LEE M. S. [ed.], 2012: Mass Spectrometry Handbook. John Wiley & Sons, Inc., Hoboken.

MACPHERSON G. J., Mittlefehldt D. W., Jones J. H., Simon S. B. [eds.], 2018: Oxygen in the Solar System. De Gruyter, Inc., Berlin.

MARTINOVSKÝ P., 2016: Environmentální bezpečnost v České republice. Masarykova univerzita, Brno.

MCCULLAGH J. et Oldham N., 2019: Mass Spectrometry. Oxford University Press, Oxford.

MEIER-AUGENSTEIN W., 2010: Stable Isotope Forensics: An Introduction to the Forensic Application of Stable Isotope Analysis. John Wiley & Sons, Inc., Hoboken.

MICHENER R. et Lajtha K., 2008: Stable Isotopes in Ecology and Environmental Science. John Wiley & Sons, Inc., Hoboken.

MISRA G. [ed.], 2019: Processing Handbook for Complex Biological Data Sources. Academic Press, London.

MOLDOVEANU S. C. et David V., 2013: Essentials in Modern HPLC Separations. Elsevier, Waltham.

MORRISON R. D. et Murphy B. L. [eds.], 2006: Environmental Forensics: Contaminant Specific Guide. Elsevier Science & Technology, London.

MURPHY B. L. et Morrison R. D. [eds.], 2007: Introduction to Environmental Forensics. Elsevier Science & Technology, London.

NAIDU R. [ed.], 2008: Chemical Bioavailability in Terrestrial Environments. Elsevier, Amsterdam.

O'NEILL P., 1998: Environmental Chemistry. Blackie Academic & Professional, London.

PÁNEK T. et Hradecký J. [eds.], 2016: Landscapes and landforms of the Czech Republic. Springer, Cham.

PAPPAS A. C., Zoidis E., Fegeros K., Zervas G., Surai P. F., 2010: Cadmium Toxicity and the Antioxidant System. Nova Science Publishers, Inc., New York.

PICO Y. [ed.], 2015: Advanced Mass Spectrometry for Food Safety and Quality. Elsevier, London.

PRASAD K., 2012: Radiation Injury Prevention and Mitigation in Humans. CRC Press, Boca Raton.

PRASAD M. N. V., Sajwan K. S., Naidu R. [eds.], 2006: Trace Elements in the Environment: Biogeochemistry, Biotechnology, and Bioremediation. CRC Press, Boca Raton.

PROHASKA T., Irrgeher J., Zitek A., Jakubowski N. [eds.], 2014: Sector Field Mass Spectrometry for Elemental and Isotopic Analysis. Royal Society of Chemistry, Cambridge.

QUEVAUVILLER P. [ed.], 2002: Methodologies for Soil and Sediment Fractionation Studies. Royal Society of Chemistry, Cambridge.

SÁŇKA M. et Materna J., 2004: Indikátory kvality zemědělských a lesních půd ČR. Ministerstvo životního prostředí, Praha.

SMITH R. M., 2004: Understanding Mass Spectra: A Basic Approach. John Wiley & Sons, Inc., Hoboken.

TENG F.-Z., Watkins J., Dauphas N. [eds.], 2017: Non-Traditional Stable Isotopes. De Gruyter, Inc., Berlin.

TOBLER E., 2019: Zinc. Enslow Publishing, LLC, New York.

USGS: U.S. Geological Survey, 2020: Mineral commodity summaries. U.S. Geological Survey, Reston.

WHITE W. M. [ed.], 2017: Encyclopedia of Geochemistry. Springer International Publishing, Cham.

Articles in scientific periodicals:

ABOUCHAMI W., Galer S. J. G., de Baar H. J. W., Middag R., Vance D., Zhao Y., Klunder M., Mezger K., Feldmann H., Andreae M. O., 2014: Biogeochemical cycling of cadmium isotopes in the Southern Ocean along the Zero Meridian. Geochimica et Cosmochimica Acta 127: 348-367.

ABOUCHAMI W., Galer S. J. G., de Baar H. J. W., Alderkamp A. C., Middag R., Laan P., Feldmann H., Andreae M. O., 2011: Modulation of the Southern Ocean cadmium isotope signature by ocean circulation and primary productivity. Earth and Planetary Science Letters 305: 83-91.

AGBENIN J. O., A De Abreu C., Van Raij B., 1999: Extraction of phytoavailable trace metals from tropical soils by mixed ion exchange resin modified with inorganic and organic ligands. Science of The Total Environment 227: 187-196.

ARNOLD T., Markovic T., Kirk G. J. D., Schönbächler M., Rehkämper M., Zhao F. J., Weiss D J., 2015: Iron and zinc isotope fractionation during uptake and translocation in rice (Oryza sativa) grown in oxic and anoxic soils. Comptes Rendus Geoscience 347: 397-404.

BALISTRIERI L. S., Borrok D. M., Wanty R. B., Ridley W. I., 2008: Fractionation of Cu and Zn isotopes during adsorption onto amorphous Fe(III) oxyhydroxide: Experimental mixing of acid rock drainage and ambient river water. Geochimica et Cosmochimica Acta 72: 311-328.

BARRAZA F., Moore R. E. T., Rehkämper M., Schreck E., Lefeuvre G., Kreissig K., Coles B. J., Maurice L., 2019: Cadmium isotope fractionation in the soil – cacao systems of Ecuador: a pilot field study. RSC Advances 9: 34011-34022.

BIGALKE M., Weyer S., Kobza J., Wilcke W., 2010: Stable Cu and Zn isotope ratios as tracers of sources and transport of Cu and Zn in contaminated soil. Geochimica et Cosmochimica Acta 74: 6801-6813.

BRAND W. A., Coplen T. B., Vogl J., Rosner M., Prohaska T., 2014: Assessment of international reference materials for isotope-ratio analysis (IUPAC Technical Report). Pure and Applied Chemistry 86: 425-467.

BRYAN A. L., Dong S., Wilkes E. B., Wasylenki L. E., 2015: Zinc isotope fractionation during adsorption onto Mn oxyhydroxide at low and high ionic strength. Geochimica et Cosmochimica Acta 157: 182-197.

CALDELAS C. et Weiss D. J., 2017: Zinc Homeostasis and isotopic fractionation in plants: a review. Plant Soil 411: 17-46.

CHAPMAN J. B., Mason T. F. D., Weiss D. J., Coles B. J., Wilkinson J. J., 2006: Chemical Separation and Isotopic Variations of Cu and Zn from Five Geological Reference Materials. Geostandards and Geoanalytical Research 30: 5-16.

COELHO C., Foret C., Bazin C., Leduc L., Hammada M., Inácio M., Bedell J. P., 2018: Bioavailability and bioaccumulation of heavy metals of several soils and sediments (from industrialized urban areas) for Eisenia fetida. Science of The Total Environment 635: 1317-1330.

DAI Y., Nasir M., Zhang Y., Wu H., Guo H., Lv J., 2017: Comparison of DGT with traditional methods for assessing cadmium bioavailability to Brassica chinensis in different soils. Scientific Reports 7: 1-9.

DEVI U. et Bhattacharyya K. G., 2018: Mobility and bioavailability of Cd, Co, Cr, Cu, Mn and Zn in surface runoff sediments in the urban catchment area of Guwahati, India. Applied Water Science 8: 1-14.

EHLERINGER J., Casale J., Lott M., Ford V., 2000: Tracing the Geographical origin of cocaine. Nature 408: 311-312.

ETTLER V., Vaněk A., Mihaljevič M., Bezdička P., 2005: Contrasting lead speciation in forest and tilled soils heavily polluted by lead metallurgy. Chemosphere 58: 1449-1459.

FANG J., Fan J. M., Lin Q., Wang Y. Y., He X., Shen X. D., Chen D. L, 2018: Characteristics of airborne lead in Hangzhou, southeast China: Concentrations, species, and source contributions based on Pb isotope ratios and synchrotron X-ray fluorescence based factor analysis. Atmospheric Pollution Research 9: 607-616.

FIJAŁKOWSKI K., Kacprzak M., Grobelak A., Placek A., 2012: The influence of selected soil parameters on the mobility of heavy metals in soils. Inżynieria i Ochrona Środowiska 15: 81-92.

FUJII T. et Albarède F., 2012: Ab Initio Calculation of the Zn Isotope Effect in Phosphates, Citrates, and Malates and Applications to Plants and Soil. PLOS One 7: 1-5.

GHOLIZADEH A., Viscarra Rossel R. A., Saberioon M., Borůvka L., Kratina J., Pavlů L., 2021: National-scale spectroscopic assessment of soil organic carbon in forests of the Czech Republic. Geoderma 385: 1-11.

GUINOISEAU D., Gélabert A., Moureau J., Louvat P., Benedetti M. F., 2016: Zn Isotope Fractation during Sorption onto Kaolinite. Environmental Science & Technology 50: 1844-1852.

HOLDEN N. E., Coplen T. B., Böhlke J. K., Tarbox L. V., Benefield J., de Laeter J. R., Mahaffy P. G., O'Connor G., Roth E., Tepper D. H., Walczyk T., Wieser M. E., Yoneda S., 2018: IUPAC Periodic Table of the Elements and Isotopes (IPTEI) for the Education Community (IUPAC Technical Report). Pure and Applied Chemistry 90: 1833-2092.

IMSENG M., Wiggenhauser M., Keller A., Müller M., Rehkämper M., Murphy K., Kreissig K., Frossard E., Wilcke W., Bigalke M., 2018: Fate of Cd in Agricultural Soils: A Stable Isotope Approach to Anthropogenic Impact, Soil Formation, and Soil-Plant Cycling. Environmental Science & Technology 52: 1919-1928.

IMSENG M., Wiggenhauser M., Müller M., Keller A., Frossard E., Wilcke W., Bigalke M., 2019: The Fate of Zn in Agricultural Soils: A Stable Isotope Approach to Anthropogenic Impact, Soil Formation, and Soil–Plant Cycling. Environmental Science & Technology 53: 4140-4149.

JEŘÁBKOVÁ J., 2019: Proč je důležitá organická hmota v půdě. Biom 1: 2.

JOUVIN D., Louvat P., Juillot F., Maréchal C. N., Benedetti M. F., 2009: Zinc Isotopic Fractionation: Why Organic Matters. Environmental Science & Technology 43: 5747-5754.

JUILLOT F., Maréchal C., Ponthieu M., Cacaly S., Morin G., Benedetti M., Hazemann J. L., Proux O., Guyot F., 2008: Zn isotopic fractionation caused by sorption on goethite and 2-Lines ferrihydrite. Geochimica et Cosmochimica Acta 72: 4886-4900.

KŘÍBEK B., Míková J., Knésl I., Mihaljevič M., Sýkorová I., 2020: Uptake of trace elements and isotope fractionation of Cu and Zn by birch (Betula pendula) growing on mineralized coal waste pile. Applied Geochemistry 122: 1-14.

KRISHNAMURTI G. S. R., Huang P. M., Van Rees K. C. J., Kozak L. M., Rostad H. P. W., 1995: Speciation of particulate-bound Cadmium of soils and its bioavailability. The Analyst 120: 659.

KRÓL A., Mizerna K., Bożym M., 2020: An assessment of pH-dependent release and mobility of heavy metals from metallurgical slag. Journal of Hazardous Materials 384: 1-9.

LI W., Gou W., Li W., Zhang T., Yu B., Liu Q., Shi J., 2019: Environmental applications of metal stable isotopes: Silver, mercury and zinc. Environmental Pollution 252: 1344-1356.

MARCHI G., Guilherme L. R. G., Chang A. C., do Nascimento C. W. A., 2009: Heavy metals extractability in a soil amended with sewage sludge. Scientia Agricola 66: 643-649.

NOVÁKOVÁ T., Kotková K., Elznicová J., Strnad L., Engel Z., Grygar T. M., 2015: Pollutant dispersal and stability in a severely polluted floodplain: A case study in the Litavka River, Czech Republic. Journal of Geochemical Exploration 156: 131-144.

PALMER M. J., Jamieson H. E., Borčinová Radková A., Maitland K., Oliver J., Falck H., Richardson M., 2021: Mineralogical, geospatial, and statistical methods combined to estimate geochemical background of arsenic in soils for an area impacted by legacy mining pollution. Science of The Total Environment 776: 1-14.

POKROVSKY O. S., Viers J., Freydier R., 2005: Zinc stable isotope fractionation during its adsorption on oxides and hydroxides. Journal of Colloid and Interface Science 291: 192-200.

POURRET O. et Bollinger J.-C., 2018: "Heavy metal" - What to do now: To use or not to use?. Science of The Total Environment 610-611: 419-420.

PUEYO M., López-Sánchez J. F, Rauret G., 2004: Assessment of CaCl2, NaNO3 and NH4NO3 extraction procedures for the study of Cd, Cu, Pb and Zn extractability in contaminated soils. Analytica Chimica Acta 504: 217-226.

QASIM B., Motelica-Heino M., Joussein E., Soubrand-Colin M., Gauthier A., 2015: Potentially toxic element phytoavailability assessment in Technosols from former smelting and mining areas. Environmental Science and Pollution Research 22: 5961-5974.

QUANTIN C., Ettler V., Garnier J., Šebek O., 2008: Sources and extractibility of chromium and nickel in soil profiles developed on Czech serpentinites. Comptes Rendus Geoscience 340: 872-882.

SCHMITT A.-D., Galer S. J. G., Abouchami W., 2009a: Mass-dependent cadmium isotopic variations in nature with emphasis on the marine environment. Earth and Planetary Science Letters 277: 262-272.

SCHMITT A.-D., Galer S. J. G., Abouchami W., 2009b: High-precision cadmium stable isotope measurements by double spike thermal ionisation mass spectrometry. Journal of Analytical Atomic Spectrometry 24: 1079-1088.

SOOTAHAR M. K., Zeng X., Su S., Wang Y., Bai L., Zhang Y., Li T., Zhang X., 2019: The Effect of Fulvic Acids Derived from Different Materials on Changing Properties of Albic Black Soil in the Northeast Plain of China. Molecules 24: 1-12.

VANĚK A., Borůvka L., Drábek O., Mihaljevič M., Komárek M., 2011: Mobility of lead, zinc and cadmium in alluvial soils heavily polluted by smelting industry. Plant, Soil and Environment 51: 316-321.

VICENTE-MARTORELL J. J., Galindo-Riaño M. D., García-Vargas M., Granado-Castro M. D., 2009: Bioavailability of heavy metals monitoring water, sediments and fish species from a polluted estuary. Journal of Hazardous Materials 162: 823-836.

WANG L., Jin Y., Weiss D. J., Schleicher N. J., Wilcke W., Wu L., Guo Q., Chen J., O'Connor D., Hou D., 2021: Possible application of stable isotope compositions for the identification of metal sources in soil. Journal of Hazardous Materials 407: 1-17.

WANG P., Li Z., Liu J., Bi X., Ning Y., Yang S., Yang X., 2019: Apportionment of sources of heavy metals to agricultural soils using isotope fingerprints and multivariate statistical analyses. Environmental Pollution 249: 208-216.

WANG P., Liu C., Yao Y., Wang C., Wang T., Yuan Y., Hou J., 2017: Comparison of in situ DGT measurement with ex situ methods for predicting cadmium bioavailability in soils with combined pollution to biotas. Water Science and Technology 75: 2171-2178.

WANG Y., Ding S., Shi L., Gong M., Xu S., Zhang C., 2017: Simultaneous measurements of cations and anions using diffusive gradients in thin films with a ZrO-Chelex mixed binding layer. Analytica Chimica Acta 972: 1-11.

WASYLENKI L. E., Swihart J. W., Romaniello S. J., 2014: Cadmium isotope fractionation during adsorption to Mn oxyhydroxide at low and high ionic strength. Geochimica et Cosmochimica Acta 140: 212-226.

WEI R., Guo Q., Yu G., Kong J., Li S., Song Z., Hu J., Tian L., Han X., Okoli C. P., 2018: Stable isotope fractionation during uptake and translocation of cadmium by tolerant Ricinus communis and hyperaccumulator Solanum nigrum as influenced by EDTA. Environmental Pollution 236: 634-644.

WIGGENHAUSER M., Bigalke M., Imseng M., Müller M., Keller A., Murphy K., Kreissig K., Rehkämper M., Wilcke W., Frossard E., 2016: Cadmium Isotope Fractionation in Soil–Wheat Systems. Environmental Science & Technology 50: 9223-9231.

WILSCHEFSKI S. et Baxter M., 2019: Inductively Coupled Plasma Mass Spectrometry: Introduction to Analytical Aspects. Clinical Biochemist Reviews 40: 115-133.

WOMBACHER F., Rehkämper M., Mezger K., Münker C., 2003: Stable isotope compositions of cadmium in geological materials and meteorites determined by multiple-collector ICPMS. Geochimica et Cosmochimica Acta 67: 4639-4654.

YANG Y., Zhang X., Liu S.-A., Zhou T., Fan H., Yu H., Cheng W., Huang F., 2018: Calibrating NIST SRM 683 as a new international reference standard for Zn isotopes. Journal of Analytical Atomic Spectrometry 33: 1777-1783.

ZALEWSKA M., 2012: Response of perennial ryegrass (Lolium perenne L.) to soil contamination with zinc. Journal of Elementology 17: 329-343.

ZHANG H., Zhao F. J., Sun B., Davison W., McGrath S. P., 2001: A New Method to Measure Effective Soil Solution Concentration Predicts Copper Availability to Plants. Environmental Science & Technology 35: 2602-2607.

ZHANG P., Yang W., Deng T., Chao Y., Wang S., Qiu R., Tang Y., 2018: Stable isotope fractionation of zinc and cadmium in soil-plant system: A review. Chinese Science Bulletin 63: 2944-2953.

ZHANG S.-N., Gu Y., Zhu Z.-L., Hu S.-H., Kopittke P.-M., Fang-Jie Zhao, Wang P., 2021: Stable isotope fractionation of cadmium in the soil-rice-human continuum. Science of The Total Environment 761: 1-8.

ZHONG Q., Zhou Y., Tsang D. C. W., Liu J., Yang X., Yin M., Wu S., Wang J., Xiao T., Zhang Z., 2020: Cadmium isotopes as tracers in environmental studies: A review. Science of The Total Environment 736: 1-9.

ZHU C., Wen H., Zhang Y., Yin R., Cloquet C., 2018: Cd isotope fractionation during sulfide mineral weathering in the Fule Zn-Pb-Cd deposit, Yunnan Province, Southwest China. Science of The Total Environment 616-617: 64-72.

Chapters in a book, articles in manuscripts:

SORIANO-DISLA J. M., Speir T. W., Gómez I., Clucas L. M., McLaren R. G., Navarro-Pedreño J., 2009: Assessment of different methods to estimate heavy metal bioavailability in 30 contrasting Spanish and New Zealand soils. In: Li L.; Kostarelos K.: EGU General Assembly Conference Abstracts. European Geosciences Union, Vienna: 4912.

VÖRÖŠ D., Geršlová E., Geršl M., Zeman J., 2015: The Distribution and Mobility of Heavy Metals in the Soils from Drahany Upland. In: Polak O., Cerkal R., Belcredi N. B. [eds.]: Mendelnet 2015. Mendel University, Brno: 604-609.

Internet sources:

ČGS: Česká geologická služba, ©2021: Geologická mapa 1:50 000 (on-line) [cit.2021.02.08], available at <https://hub.arcgis.com/datasets/0442952541704ae9b488c59cec92c2b4?layer =2>.

ČÚZK: Český úřad zeměměřický a katastrální, ©2021: Základní báze geografických dat České republiky (ZABAGED®) [cit.2021.02.08], available at: <http://ags.cuzk.cz/arcgis>.

SERC: Carleton's Science Education Resource Center (SERC), ©2007: Mass Spectrometry Schematic (on-line) [cit. 2020.09.27], available at <https://serc.carleton.edu/details/images/9094.html>.

Legislative materials:

DECREE No. 153/2016 Coll., decree on the determination of details of the protection of the agricultural land's quality, as amended.

Technical standards:

BS ISO 10390:2005: Soil quality — Determination of pH. BSI, London, 2005. 14.

USEPA SW-846 Test Method 3052: Microwave Assisted Acid Digestion of Siliceous and Organically Based Matrices. US EPA, Washington, D.C., 1996. 20.